Megataxa 019 (1): 176–212
https://www.mapress.com/mt

Article

ISSN 2703-3082 (print edition)
MEGATAXA
ISSN 2703-3090 (online edition)

https://doi.org/10.11646/megataxa.19.1.3
http://zoobank.org/urn:lsid:zoobank.org:pub:F75DF96E-265B-4EFF-9EF3-F6213DAB200F

Zigzags in the White Sand Belt: A new, highly divergent lineage of sand-swimmer skink from Madagascar (Squamata: Scincidae)

AURÉLIEN MIRALLES[1,2*], ROBIN SCHMIDT[2], FRANCESCO BELLUARDO[3], NY ANDO RAHAGALALA[4], EVARISTE MONVOISIN[5], FANOMEZANA M. RATSOAVINA[4], JÖRN KÖHLER[6], FRANK GLAW[7] & MIGUEL VENCES[2]

[1]*Institut de Systématique, Évolution, Biodiversité (ISYEB), Muséum national d'Histoire Naturelle, CNRS, Sorbonne Université, EPHE, Université des Antilles, 57 rue Cuvier, 75231 Paris cedex, France*
miralles.skink@gmail.com; https://orcid.org/0000-0002-2538-7710
[2]*Zoological Institute, Braunschweig University of Technology, Mendelssohnstr. 4, 38106 Braunschweig, Germany*
robin.schmidt@tu-braunschweig.de; https://orcid.org/0000-0003-1269-2553
m.vences@tu-braunschweig.de; https://orcid.org/0000-0003-0747-0817
[3]*EnviXLab, Department of Biosciences and Territory, University of Molise, Contrada Fonte Lappone s.n.c., 86090 Pesche, Italy*
france89belluardo@gmail.com; https://orcid.org/0000-0002-3967-2686
[4]*Mention Zoologie et Biodiversité Animale, Université d'Antananarivo, BP 906, Antananarivo, 101 Madagascar*
nyando.andrea@gmail.com; https://orcid.org/0009-0006-7238-9993
fanomezanarts@gmail.com; https://orcid.org/0000-0003-1661-1669
[5]*Direction générale déléguée aux collections (DGD.C), Muséum national d'Histoire Naturelle, 57 rue Cuvier, 75231 Paris cedex, France*
evariste.monvoisin2@mnhn.fr; https://orcid.org/0009-0002-3680-998X
[6]*Hessisches Landesmuseum Darmstadt, Friedensplatz 1, 64283 Darmstadt, Germany*
joern.koehler@hlmd.de; https://orcid.org/0000-0002-5250-2542
[7]*Zoologische Staatssammlung München (ZSM-SNSB), Münchhausenstr. 21, 81247 München, Germany*
glaw@snsb.de; https://orcid.org/0000-0003-4072-8111
** Corresponding author*

Abstract

The present work reports on the discovery of a new sand swimming lizard (Scincidae: Scincinae) in Madagascar. This limbless and eyeless skink was found during fieldwork in the northern part of the "great white sand belt", a series of patchy white sand areas encircling the island's western sedimentary basins. The new taxon shows a distinctive combination of derived morphological traits (miniaturized, limbless, elongated body, with absent or scale-covered eyes and ear openings, and a reduced head scale pattern) reminiscent of other Malagasy fossorial skinks adapted to sandy habitats (e.g. *Voeltzkowia*, *Grandidierina* and some *Paracontias*). Phylogenetic analyses based on two datasets (multilocus DNA from Sanger sequencing and genome-wide DNA sequences derived from double-digest Restriction Associated DNA [ddRAD]) reveal a highly divergent phylogenetic position of this taxon and, given its distinct morphology, justify its description as a new species in a new genus, *Zig zag* **gen. nov.** & **sp. nov.** This marks the first genuine field discovery of a new genus of Scincidae in Madagascar since the 19th century, i.e., the discovery of a formerly unknown deep clade rather than an identification (and split) from an already recognized genus. Our results also shed light on the ancient evolutionary history of this taxon and its sister clade, *Paracontias*. Finally, the present work explores the factors that may explain why ecosystems characterized by white sand substrates, an ecosystem often neglected in biodiversity research, but present in various regions of the globe (e.g., Florida sand scrub, South American WS savannah, Indonesian Keranga) have seemingly so frequently promoted the convergent evolution of fossorial squamates.

Key words: Taxonomy, new genus, new species, Phylogenomics, psammophily, fossoriality

Introduction

Often depicted as the eighth continent, Madagascar and its satellite islands represent a global biodiversity hotspot. This isolated region in the Indian Ocean is also characterized by extraordinary rates of endemism, with more than 90% of species of vertebrates and 82% of flowering plants occurring nowhere else in the world (Antonelli *et al.* 2022). Its diversified reptile fauna is in line with this trend, with ~460 described species recognized to date, of which more than 98% endemic to this island

 Submitted: 14 Oct. 2025; accepted by Z.-Q. Zhang: 1 Feb. 2026; published: 23 Jan. 2026

nation (Uetz 2025). The number of recognized species of Malagasy Squamata is constantly increasing, and the absence of any sign of a slowdown in the discovery rates suggests that many more have yet to be described (Fig. 1A; Uetz 2025).

Within Madagascar's lizard diversity, the skink family (Scincidae) represents the second most species-rich group after geckos (Gekkonidae), with 81 species currently recognized (Uetz 2025; Miralles *et al.* 2025). The pace of species discovery in skinks mirrors that of other Malagasy squamates, showing two distinct historical phases marked by periods of intensive taxonomic progress: The first phase started in the period of the great naturalist explorations of the 19th century (Duméril & Bibron 1839; Peters 1854; Grandidier 1867, 1869, 1872 ; Günther 1877; O'Shaughnessy 1879; Peters

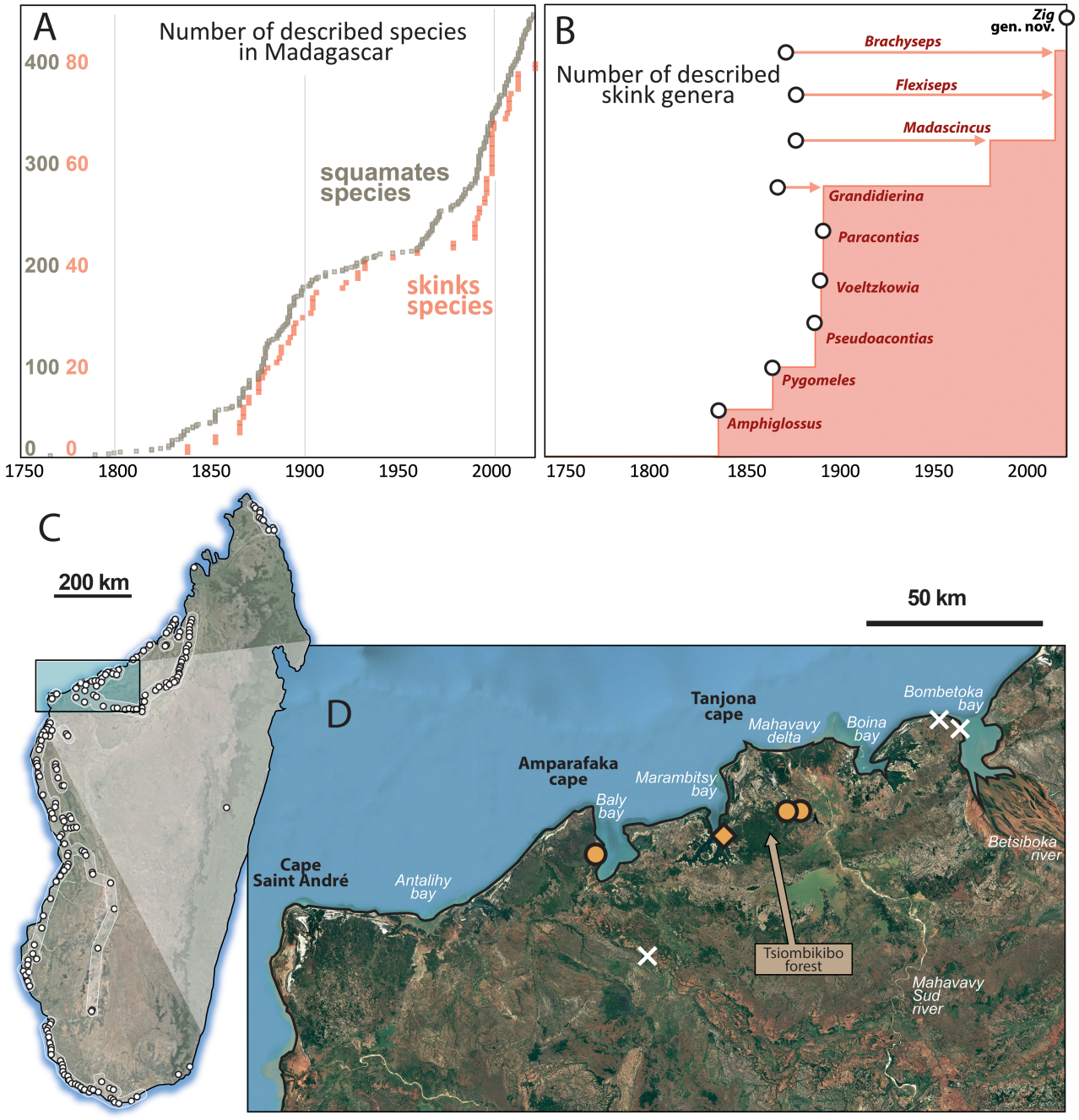

FIGURE 1. Diagrams showing temporal trends in the description of (A) scincine skink species and (B) genera from Madagascar, based on currently recognized taxa in the Reptile Database (Uetz 2025), excluding synonymized genera. In B, the white circles indicate the years of description of the type species for each of these corresponding genera (instead of the year of description of each genus), thereby providing a more precise account, over time, of the accumulation of "new deep lineages" discovered. (C) Map of Madagascar indicating the great white sand belt, with dots marking white sand areas identified by Miralles *et al.* (2025). (D) Map of coastal area in Northwest Madagascar indicating known localities of *Zig zag* **gen. nov. & sp. nov.** (orange dots for the sequenced material and a diamond for Antsakoamanery which is based on UMMZ specimens examined based on photographs). White crosses indicate surveyed white sand areas where the species was not found; large areas near Cap Saint André remain unprospected.

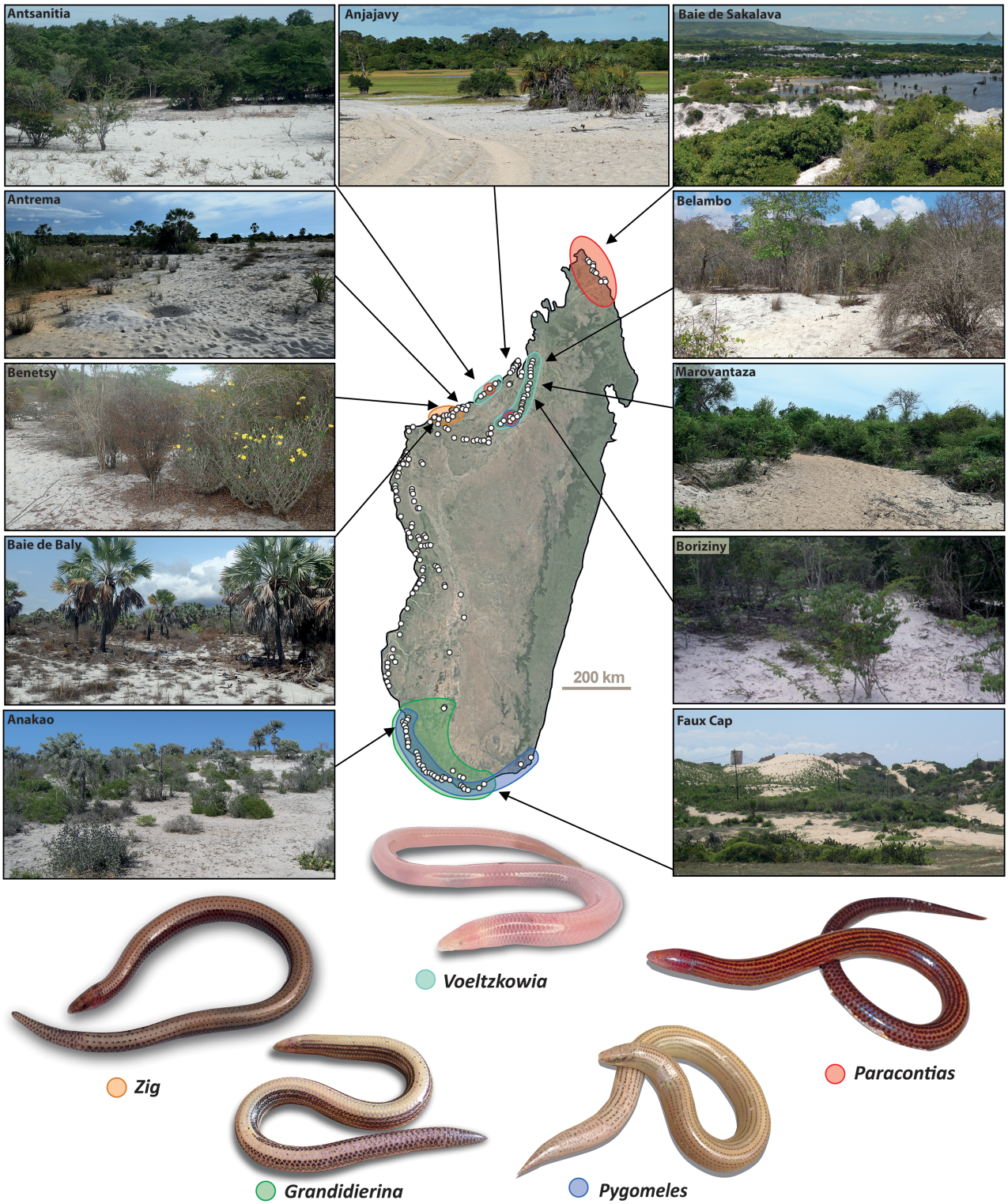

FIGURE 2. Overview of the White Sand Belt: Map of Madagascar showing WS patches identified by Miralles *et al.* (2025) (white dots), with the distribution of sand-specialist, legless and fossorial skink genera (data from the present study; Glaw & Vences 2007; Köhler *et al.* 2010; Miralles *et al.* 2011b, 2015, 2016a, 2025).

1880; Boettger 1881, 1882, 1893; Boulenger 1887, 1888, 1889, 1896; Bocage 1889; Mocquard 1894, 1897, 1901, 1905, 1906a, 1906b, 1908), while the 20th century saw a marked slowdown in the description rate (Sternfeld 1918; Kaudern 1922; Angel 1924, 1930, 1934, 1949; Pasteur & Paulian 1962; Brygoo 1981). The second phase, notably favored by the development of molecular taxonomy, was driven by a revitalized research activity in the 1990s and continues up to this day (Raxworthy & Nussbaum 1993; Nussbaum & Raxworthy 1994, 1995a, 1995b, 1998a, 1998b; Nussbaum *et al.* 1999; Ramanamanjato *et al.* 1999a, 1999b; Andreone & Greer 2002; Sakata & Hikida 2003a, 2003b; Köhler *et al.* 2009, 2010; Miralles *et al.* 2011a, 2011b, 2011c, 2012, 2016a, 2016b, 2025).

In contrast to the steady increase in species, the number of currently recognized scincid genera in Madagascar has changed very little since the beginning of the 20th century, increasing from six to only nine in the subfamily Scincinae. Among the currently recognized genera, only three genera (*Madascincus* Brygoo, 1981, *Flexiseps* Erens *et al.*, 2017, and *Brachyseps* Erens *et al.*, 2017) have been described since 1900, and all three of these new genera resulted from the partitioning of already described ones. This would suggest that all the major clades at the genus level (i.e., genus-level or higher) composing the Malagasy scincine radiation would have been collected already long time ago (Fig. 1B). Contrary to this expectation, the present study demonstrates that at least one previously unreported deeply divergent clade still exists in the extant herpetofauna of Madagascar.

Numerous new scincine discoveries, including the one reported herein, are arising from recent fieldwork conducted in specific areas of the North West of Madagascar (*sensu* Boumans *et al.* 2007). This collection campaign focused on the investigation of patchy white sand (WS) areas that span across the island from north to south over a distance of more than 1500 km and encircle, along the coast and further inland, the main sedimentary basins of the island's western coast. This two-layer "belt of white sand" consists of an inland corridor that appears to have formed by the erosion of older, consolidated white continental sandstones. In contrast, the sand of the coastal corridors likely originated from these inland sandstones and was transported over short distances by Madagascar's rivers (Fig. 2, see also Miralles *et al.* 2025 for more details). In this area, especially the Mahajanga basin is known to harbor a wide variety of micro-endemic sand fossorial species—here termed "sand swimmers" based on their highly specialized habits—many of which were only recently discovered (see for instance Sakata & Hikida 2003b; Miralles *et al*. 2012, 2016a). Our recent fieldwork revealed the existence of two new species of *Voeltzkowia* from the Bongolava massif (Miralles *et al.* 2025), but more interestingly also resulted in the collection of a third undescribed species, difficult to assign to any known genus.

The newly encountered skink exhibits a peculiar mosaic of derived morphological traits (including a miniaturized, limbless and very elongated body, the lack of eyes and ear openings, and particular head scale fusions) that are reminiscent of, but do not fully match, the character states of other Malagasy fossorial skinks highly adapted to sandy areas, such as *Voeltzkowia*, *Grandidierina, Pygomeles* and some *Paracontias* species. The present work aims at elucidating the phylogenetic position of this new taxon, by combining evidence from DNA sequences obtained by Sanger sequencing of multiple gene fragments, and by genome-wide double-digest restriction-associated DNA sequencing (ddRADseq). Our data reveal that the collected skinks represent not only a new species but based on their high genetic divergence and morphological distinctiveness, a new genus. We here formally name and describe this peculiar taxon and discuss aspects related to its ancient evolutionary origin.

Materials and methods

For the sake of simplicity and clarity, we will anticipate our taxonomic results and introduce from here on the name of the new taxon described as *Zig zag* **gen. nov.** & **sp. nov.** herein. Its formal description is presented below in the taxonomy section.

Sampling localities and acronyms

Sampling campaigns were carried out in March and October 2023 in order to explore various white sand areas around the Mahajanga basin (Miralles *et al.* 2025). In the western part of the basin (i.e., East side of the Betsiboka river), fieldwork took place at Ambararata (midway between Soalala and Namoroka, 16.30426°S, 45.38372°E), Antrema (15.71144°S, 46.17491°E), Baie de Baly National Park, near the village of Baly (16.05194°S, 45.27119°E), Tsiombikibo forest, near the village of Benetsy (15.93936°S, 45.77064°E) and Katsepy (15.75912°S, 46.24318°E). The acronyms MIRZC and FGZC correspond to the field number series of Aurélien Miralles and Frank Glaw, respectively. Morphological data were derived from voucher specimens deposited in the herpetological collections of the Muséum National d'Histoire Naturelle, Paris, France (MNHN), Mention Zoologie et Biodiversité Animale of the University of Antananarivo, Madagascar (UADBA), and Zoologische Staatssammlung München, Germany (ZSM). Data of specimens from the Museum of Zoology, University of Michigan, USA (UMMZ) were retrieved from their database (https://lsa.umich.edu/ummz/herps.html). Specimens in the UADBA collection have in many cases not yet been provided with final catalogue numbers but are identifiable by their field number tags. Therefore, we report these specimens as UADBA-FGZC (for specimens with FGZC field numbers).

Morphology

Newly collected specimens were euthanized by intra-coelomic (IC) injection of 250–500 mg/kg pH-neutralized 1% MS-222, followed by 0.5–1 ml 50% unbuffered MS-222 (Conroy *et al.* 2009), then fixed in 90% ethanol and preserved in 70% ethanol. Specimens used for comparisons are listed in Appendix 1. All measurements

were recorded by AM to the nearest 0.1 mm using a dial caliper. Meristic, mensural and qualitative characters examined here are routinely used in the taxonomy of Scincidae, such as scale counts or presence/absence of fusions of homologous scales. Scale nomenclature, scale counts, and measurements used in the morphological analyses essentially follow Miralles *et al.* (2016a).

In herpetological literature, the term *fusion* of scales commonly refers to an evolutionary transition from a condition with two or more small scales to one with a single larger scale occupying approximately the same position, shape, and extent—and thus presumed to be homologous to the smaller scales. The inverse evolutionary transformation is referred to as *fragmentation*. In this study, we chose to continue using these terms for practical reasons. It is nevertheless essential to emphasize that these terms (*fusion* and *fragmentation*) do not imply any specific morphogenetic processes but refer solely to evolutionary transitions from one state to another, regardless of the ontogenetic mechanisms involved.

The term "*blind"* is used herein to describe lidless species, with non-opening eyes that are significantly reduced in size and deeply sunken beneath a semi-translucent ocular scale. It makes no assumption about the visual acuity or photosensitivity of these organisms, which have not yet been studied in this regard.

Except for the new taxon *Zig zag* **gen nov.** & **sp. nov.**, the numbers of presacral vertebrae given herein (i.e., for various species of *Paracontias*) were taken from the literature (Brygoo 1980; Andreone & Greer 2002; Köhler *et al.* 2009, 2010).

Micro-computed tomography

One *Zig zag* **gen nov.** & **sp. nov.** specimen (holotype MNHN-RA-2025.0001) was scanned three times using an Easytom S 130 Micro-CT : at 106 µA, 75 keV and a resolution (voxel size) of 15 µm (whole specimen—five stacks, each consisting of 768 images) and at 110 and 88 µA, 80 keV and a resolution of 6 µm (anterior part of the body—one stack of 1248 images, and pelvic region—one stack of 960 images, respectively). Projection data were reconstructed into a volumetric dataset using UniCT Xact software (version 23.04, revision 2023-06-27). The resulting volume was then analyzed using Dragonfly software (version 2024.1.0.1613) to generate a complete osteological mesh of the skeleton. The isolated skeletal mesh underwent optimization—including decimation, smoothing, and centering—using Geomagic Wrap software (version 2021.2.2.3022).

Sanger sequencing and DNA sequence analysis

We selected four samples of the new taxon (two from Baly and two from Benetsy) for PCR amplification and Sanger sequencing of DNA fragments of two mitochondrial genes (16S rRNA 3' terminus and 12S rRNA, abbreviated 16S and 12S) and four nuclear-encoded markers (brain-derived neurotrophic factor, BDNF; Phosducin, PDC; recombination activating gene 2, RAG2; and oocyte maturation factor, CMOS). For PCR primers and laboratory protocols, see Erens *et al.* (2017) and Belluardo *et al.* (2023). We combined the new sequences with the dataset of Belluardo *et al.* (2023), which itself integrated newly determined sequences with those from previous works (Schmitz *et al.* 2005; Crottini *et al.* 2009; Nagy *et al.* 2012; Miralles & Vences 2013; Miralles *et al.* 2015, 2016a, 2016b; Erens *et al.* 2017). The resulting supermatrix, designed to represent the species diversity of Malagasy scincines, was composed of 74 samples (70 ingroup and 4 outgroup samples, representing 45 ingroup species and the nine genera recognized so far, plus the new genus *Zig*) and 14 gene fragments in total, with four mitochondrial gene fragments (12S, 16S, cytochrome oxidase subunit I, COI, and NADH-dehydrogenase subunit 1 with adjacent tRNAs, ND1), and 10 nuclear-encoded gene fragments (BDNF, CMOS, PDC, RAG1, RAG2, alpha-enolase (ENO1), two non-overlapping segments of sacsin (SACS-A and SACS-B), leucine-rich repeat and WD repeat-containing protein (KIAA1239), and titin (TTN)). Additionally, a 16S fragment was sequenced for all the 18 newly collected samples. These sequences were aligned and used to calculate uncorrected *p*-distances, and to produce a neighbor-joining distance tree with MEGA 11 to visualize their genetic differentiation (Tamura *et al.* 2021). Forty-one new sequences were submitted to GenBank (accession numbers PX841715–PX841718, PX843754–PX843774, PX843775–PX843778, PX868793–PX868804); all sampling details and GenBank accession numbers are available in Table 1).

Input files for phylogenetic analysis of the multigene supermatrix were prepared with PipeLogeny in R 4.4.1 (Muñoz-Pajares *et al.* 2019; R Core Team 2024). Starting from the concatenated multilocus matrix, sequences were aligned with MAFFT 7.310 (Katoh & Standley 2013). The optimal partitioning scheme and models of evolution were determined with PartitionFinder 2.1.1 (Lanfear *et al.* 2016) using the Bayesian Information Criterion for model selection. A phylogenetic tree was reconstructed using Bayesian Inference (BI) implemented in MrBayes 3.2.7a (Ronquist *et al.* 2012). Specifically, two independent runs of 50 million sweeps of the Markov Chain Monte Carlo (MCMC) chain, each consisting of four chains, were executed with 40% burn-in and MCMC chain sampling at every 1,000 generations. Run convergence and parameter posterior distributions were assessed in Tracer 1.7.1 (Rambaut *et al.* 2018), considering a minimum threshold of Effective Sampling Size of 200.

In addition to the concatenated multilocus phylogeny, a species tree was inferred using ASTRAL 5.7.8 (Zhang *et al.* 2018) from gene trees inferred from each of the 10 nuclear markers and a single gene tree inferred from a concatenated alignment of the four mitochondrial markers. Gene trees were inferred following the same procedure as for the concatenated multilocus phylogeny, except that MrBayes was run for 20 million MCMC generations. ASTRAL was executed with default parameters on the 50%-majority rule consensus trees of each gene tree.

Divergence times were estimated with BEAST 2.6.0 (Bouckaert *et al.* 2019) on the same concatenated multilocus supermatrix used to infer BI tree, following the settings of Belluardo *et al.* (2023), who reconstructed

a dated phylogeny from the same matrix (without the sequences of the new genus added in the present study). Specifically, we applied the following settings: 1) substitution models as defined in the optimal partitioning scheme for the BI tree; 2) a relaxed lognormal clock with exponential priors for ucldMean (mean = 0.05) and ucldStdev (mean = 0.3333); 3) a Birth-Death speciation model with default parameters; 4) topological constraints on the Malagasy Scincinae crown node and the clade *Amphiglossus-Brachyseps-Flexiseps-Pygomeles-Voeltzkowia*; 5) calibration of the Malagasy Scincinae crown node using a normal prior distribution with an offset equal to the average height of the same node used in Belluardo *et al.* (2023) (56.8204 million years ago (Ma)), with mean equal to 0 and sigma equal to 10.7 to match the 95% Higher Posterior Density Interval (HPDI) of the same time estimate. We executed two independent runs in BEAST, each consisting of 30 million MCMC steps. Run convergence was assessed with Tracer, and tree posterior distributions were combined in LogCombiner 2.6.0 (Bouckaert *et al.* 2019) with a 40% burn-in. The maximum clade credibility tree was generated with TreeAnnotator 2.6.0 (Bouckaert *et al.* 2019).

Relationships between alleles (haplotypes) of the four nuclear-encoded gene fragments in the new taxon were visualized as haplotype genealogies (networks). BDNF, CMOS, RAG2 and PDC alignments were trimmed to equal length of all sequences, respectively, by removing regions of poor quality and sequences with missing data. Alleles were then inferred using the PHASE algorithm (Stephens *et al.* 2001) implemented in the software Hapsolutely (Vences *et al.* 2024), and haplotype genealogies following the Fitch tree algorithm (Salzburger *et al.* 2011; Matschiner 2016) were inferred using the same program.

Restriction-associated DNA sequencing

We selected 48 samples of 17 ingroup species (of the nine Malagasy scincine genera recognised so far, plus the new genus), in order to represent the genus level diversity within Malagasy scincines for phylogenomic analysis. These samples were submitted to ddRAD sequencing following an adapted version of the protocol of Brelsford *et al.* (2016) (dx.doi.org/10.17504/protocols.io.kxygx3nzwg8j/v1). Library preparation consisted of restriction enzyme digestion with MseI and SbfI, ligation of individual unique barcodes, PCR amplification, a size selection of the ligated fragments (between 400 and 500 bp) by performing a gel extraction using the Monarch DNA Gel Extraction Kit (New England Biolabs), and paired end sequencing of the purified library on an Illumina NextSeq using a 2 × 75 bp kit (two lanes/library).

Raw reads were processed with Stacks v2.61 (Catchen *et al.* 2013; Rochette *et al.* 2019), which includes demultiplexing, data filtering, and trimming to 65 bp (module *process_radtags*), de novo assembling, cataloging, and SNP calling (module *denovo_map.pl*), as well as SNP filtering for downstream analyses (module *populations*). The Stacks catalog contained 496,735 loci with a mean effective per-sample coverage of 32.2x. Default stacking parameters (-m, -n and -M) were applied, following the suggestions by Paris *et al.* (2017). For each sub-dataset, the filtering options (-p and -r) were optimized to achieve a balance between the number of loci and missing data across all species. Raw reads were submitted to the NCBI Short Read Archive under Bioproject PRJNA1333502 (see Appendix 2 and Miralles *et al.* 2025 for more details).

Within the *populations* module, the *-phylip-var-all* option of Stacks v2.61 was employed to export alignments for each dataset. Subsequently, Maximum likelihood

TABLE 1. List of samples used in molecular analyses. The table lists all the tissue samples and newly generated Sanger sequences of *Zig zag* **gen nov.** & **sp. nov.**. For more details concerning the complementary samples (samples of species from other genera) used in the concatenated multilocus analyses, see Belluardo *et al.* (2023). ddRADseq raw reads (Biosamples) were submitted to the NCBI Short Read Archive under Bioproject PRJNA1333502 (see Miralles *et al.* 2025 for more details). HT: Holotype; PT: Paratypes.

Locality	**Voucher**	**sample**	ddRAD	16S	12S	BDNF	PDC	RAG2	CMOS
Baly	ZSM 101/2023, PT	FGZC 12001	SAMN51797855	PX843774	-	-	-	-	-
Baly	ZSM 102/2023, PT	FGZC 12004	SAMN51797856	PX843773	-	-	-	-	-
Baly	MNHN-RA-2025.0001, HT	FGZC 12006	SAMN51797857	PX843772	PX843778	PX868803	PX868795	PX868799	PX841718
Baly	ZSM 104/2023, PT	FGZC 12020	SAMN51797859	PX843770	PX843777	PX868804	PX868796	PX868800	PX841717
Baly	UADBA	FGZC 12019	SAMN51797858	PX843771	-	-	-	-	-
Baly	Not collected	MIRZC 1241	-	PX843769	-	-	-	-	-

.....continued on the next page

TABLE 1. (Continued)

Locality	Voucher	sample	ddRAD	16S	12S	BDNF	PDC	RAG2	CMOS
Baly	Not collected	MIRZC 1242	-	PX843768	-	-	-	-	-
Baly	Not collected	MIRZC 1245	-	PX843767	-	-	-	-	-
Baly	Not collected	MIRZC 1246	-	PX843766	-	-	-	-	-
Benetsy	ZSM 105/2023, PT	FGZC 12025	SAMN51797860	PX843761	PX843776	PX868802	PX868794	PX868797	PX841716
Benetsy	ZSM 106/2023, PT	FGZC 12026	SAMN51797861	PX843760	PX843775	PX868801	PX868793	PX868798	PX841715
Benetsy	ZSM 107/2023, PT	FGZC 12027	SAMN51797862	PX843759	-	-	-	-	-
Benetsy	ZSM 113/2023, PT	FGZC 12053	SAMN51797866	PX843754	-	-	-	-	-
Benetsy	UADBA	FGZC 12034	-	PX843762	-	-	-	-	-
Benetsy	UADBA	FGZC 12052	SAMN51797865	PX843757	-	-	-	-	-
Benetsy	UADBA	FGZC 12033	-	PX843763	-	-	-	-	-
Benetsy	UADBA	FGZC 12023	-	PX843765	-	-	-	-	-
Benetsy	Not collected	MIRZC 1248	-	PX843755	-	-	-	-	-
Benetsy	ZSM 108/2023, PT	FGZC 12028	SAMN51797863	PX843758	-	-	-	-	-
Benetsy	Not collected	MIRZC 1251	-	PX843756	-	-	-	-	-
Benetsy	ZSM 109/2023, PT	FGZC 12029	SAMN51797864	-	-	-	-	-	-
Benetsy	ZSM 110/2023, PT	FGZC 12030	-	PX843764	-	-	-	-	-

(ML) phylogenies were reconstructed using IQTree v2.2.0 (Minh *et al.* 2020). The best substitution model for each dataset was determined using the integrated ModelFinder (Kalyaanamoorthy *et al.* 2017), and branch support was assessed through 1,000 replicates of ultrafast bootstraps (UFBoot; Hoang *et al.* 2018) and 1,000 replicates of SH-like approximate likelihood ratio tests (SH-aLRT; Guindon *et al.* 2010). The raw trees were rooted and visualized using FigTree v1.4.4 (Rambaut 2010) and further refined in Adobe Illustrator.

Analyses of character evolution

The evolutionary history of a single ecological trait (substrate preference) was reconstructed across the phylogenetic tree of the limbless clade formed by *Zig* **gen. nov.** and *Paracontias* clade (*ZiPa* clade). Following Andreone & Greer 2002; Glaw & Vences 2007; Köhler *et al*. 2009, 2010; Miralles *et al*. 2011b, 2016a and the present study, two distinct ecological states were defined: (1) the *psammophilous state* (sand affinity), which includes species typically associated with predominantly mineral, sandy substrates (most often white sand) found in northern and north-western Madagascar, usually in dry deciduous forests or bushy savannah-like vegetations (i.e. *P. ampijoroensis*, *P. fasika*, *P. mahamavo*, *P. minimus*, *P. rothschildi* and *Zig zag* **gen. nov. & sp. nov.**); and (2) the *humicolous state* (humus affinity), referring to species primarily found in moist evergreen forests, where they inhabit mainly organic substrates such as decomposing leaf litter (i.e. *P. brocchii*, *P. hafa*, *P. holomelas*, *P. kankana*, *P. manify*, *P. milloti*, *P. tsararano* and *P. vermisaurus*). See Appendix 2 for more details.

Character state reconstructions were performed using two distinct approaches, the first based on a deterministic conceptual framework (Maximum Parsimony), the second on a probabilistic framework (Maximum Likelihood):

Maximum parsimony reconstructions (MP) were implemented in Mesquite 3.81 (Maddison & Maddison

2023) with default settings and using the topology obtained from the concatenated multilocus bayesian inference. Maximum likelihood analyses (ML) were implemented using the 'Hidden State Speciation and Extinction' (HiSSE) approach implemented in the R package hisse 2.1.11 (Beaulieu & O'Meara 2016). HiSSE incorporates unobserved (hidden) states that may affect both diversification and transition rates associated with the observed states (psammophilous vs humicolous substrate preference). We tested a set of 24 models encompassing various combinations of hidden states and including 'Binary-State Speciation and Extinction' (BiSSE) models (Maddison *et al.* 2007), which account exclusively for the diversification dynamics associated with the two observed states (more details in Appendix 3). We performed model-testing analyses on a set of 50 posterior trees randomly sampled from the posterior distribution of the dated phylogeny (see Sanger sequencing and DNA sequence analysis). The model resulting as the best-fitting over the majority of the sampled trees based on AICc weights (Burnham & Anderson 2002) was fitted to the maximum clade credibility tree of the dated phylogeny for the ancestral state reconstruction performed with the same R package.

Nomenclatural acts

The electronic edition of this article conforms to the requirements of the amended International Code of Zoological Nomenclature, and hence the new names contained herein are available under that Code from the electronic edition of this article. This published work and the nomenclatural acts it contains have been registered in ZooBank, the online registration system for the ICZN. The LSID (Life Science Identifier) for this publication is: lsid:zoobank.org:pub:F75DF96E-265B-4EFF-9EF3-F6213DAB200F. Raw data, alignments, treefiles and supplementary information are available from https://doi.org/10.5281/zenodo.17145228.

Results

Field prospection

Specimens of sand-swimming skinks allocated to the new taxon were collected at two sites, Benetsy and Baie de Baly, but not in other white sand areas prospected in the wider area (i.e. Antrema, Katsepy and Ambararata; Fig. 1D). In these three localities, the absence of sinusoidal tracks in the sand (present in high density in localities where the species was found) suggests this species is likely absent.

Molecular phylogenetic analyses

The molecular data unanimously suggest that the new taxon represents a distinct lineage which is highly divergent from all other Malagasy scincines. This is supported both by the RADseq data (2,031 loci, 24,842 SNPs, total alignment length of 258,554 bp, Fig. 3A), and by the two trees based on the Sanger sequence dataset (concatenated multilocus BI (Fig. 3B) and ASTRAL species tree (Fig. 4A), total alignment length of 10,416 bp). For more clarity, a comparative overview of the three alternative topologies obtained is also provided in Figure 4B. The three analyses strongly support that (1) *Zig zag* **gen. nov. & sp. nov.** is nested within clade A (*sensu* Crottini *et al.* 2009; Erens *et al.* 2017; Belluardo *et al.* 2023), and that (2) all the genera of Malagasy scincines are reciprocally monophyletic (with the sole exception of *Flexiseps* in the species tree). These trees also unambiguously agree on (3) the monophyly of clade B (formed by *Amphiglossus*, *Brachyseps*, *Flexiseps, Grandidierina*, *Voeltzkowia* and *Pygomeles*) and (4) the branching of *Pseudoacontias* from a very basal node (i.e. potentially forming a third major clade C distinct from the two others). The RADseq tree and the concatenated multilocus tree agree on the placement of *Zig* **gen. nov.** as sister group of *Paracontias* (support of 1.0 and 0.85, respectively). In contrast, the species tree supports a closer relationship of *Zig* **gen. nov.** with *Madascincu*s, but with very weak support (0.58). Disagreements of the three trees include (1) the exact position of *Pseudoacontias*, which is either recovered as the sister group to the clade B (RADseq tree and species tree, with full and very low support, respectively) or as the sister clade to all the other Malagasy scincine skinks (concatenated multilocus tree, with full support), (2) the monophyly of the genus *Flexiseps* (recovered as two distinct clades in the species tree only), (3) and on the relationships between the genera included in clade B, especially regarding the position of *Grandidierina* which splits from a basal node within clade B in the concatenated multilocus tree but is sister to *Brachyseps* in the other two trees.

Genetic divergences (uncorrected p-distances of the 16S mtDNA fragment) between *Zig zag* **gen. nov. & sp. nov.** and species of *Paracontias* range from 5.5 to 8.8% (mean=6.9%) and those between *Zig zag* **gen. nov. & sp. nov.** and *Madascincus* species range from 4.7 to 8.8% (6.9%). These values are very similar to those calculated between members of the genera *Paracontias* and *Madascincus,* which range from 4.2 to 10.9% (7.0%).

Regarding the intraspecific differentiation within *Zig zag* **gen. nov. & sp. nov.**, both the RADseq and Sanger sequence-based approaches robustly agree on the reciprocal monophyly of the Baly Bay and Benetsy populations. The uncorrected p-distances of the 16S mtDNA fragment range from 0 to 0.2% within each population, and from 0.6 to 1.0% between both populations (Fig. 5B1). Haplotype genealogies reconstructed from fragments of the four nuclear-encoded genes show a very low overall allelic diversity, with only two different haplotypes for PDC and CMOS (with one and two mutational steps distinguishing them, respectively), and a unique common haplotype for BDNF and for RAG2 (Fig. 5B2). Among the two polymorphic nuclear loci identified, only one, CMOS, presents diagnostic haplotypes unambiguously differentiating each population.

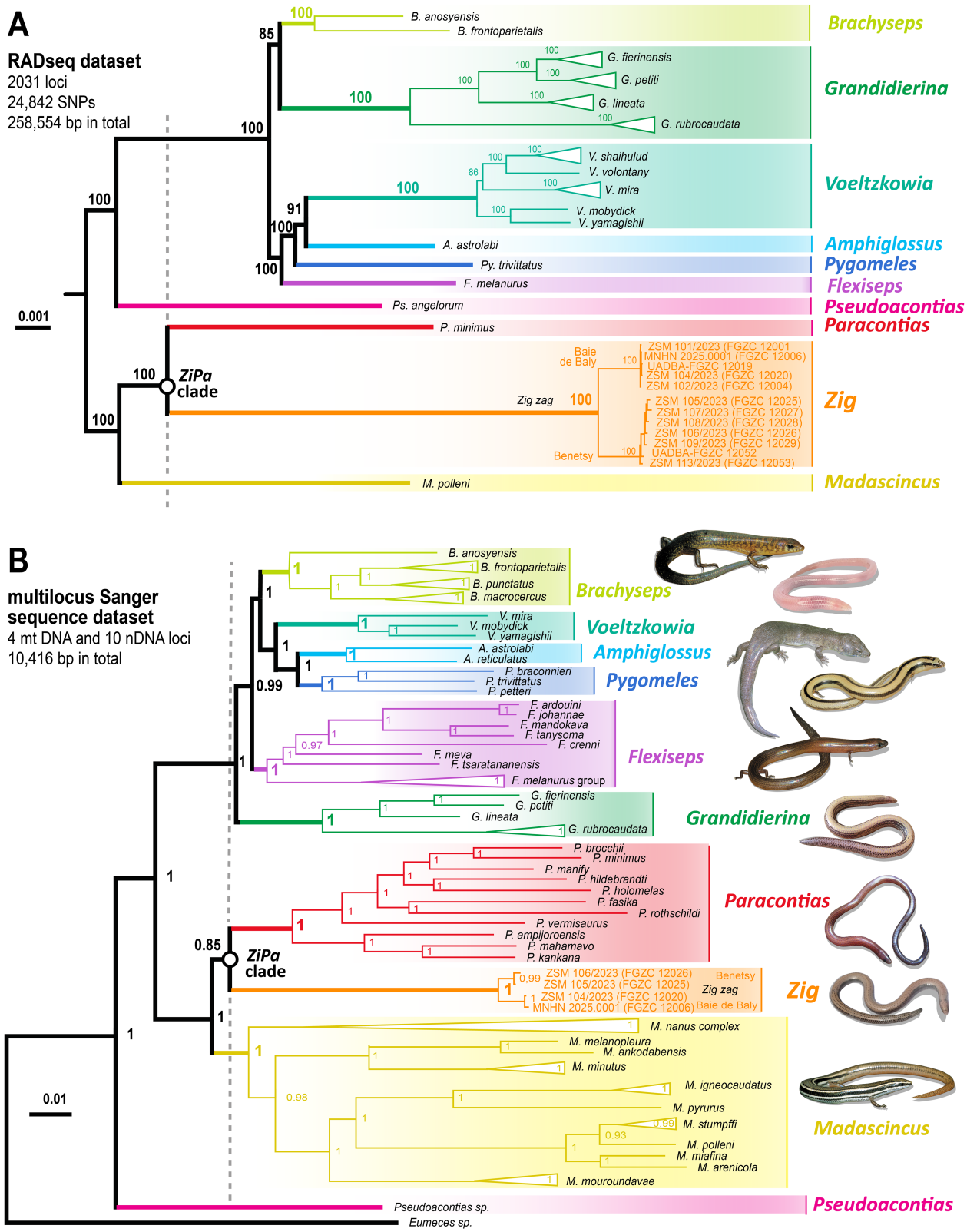

FIGURE 3. (A) Phylogenomic ddRADseq tree and (B) Bayesian phylogenetic tree (50%-majority rule consensus tree) based on the concatenated alignment of the supermatrix of DNA sequences from 14 mitochondrial and nuclear gene fragments obtained by Sanger sequencing. The vertical dotted line is used to highlight the relative depth of the *Zig* **gen. nov.** clade (i.e. divergence from its sister clade), compared to other genus-level clades. Terminal triangles represent species-level clades collapsed for the sake of clarity.

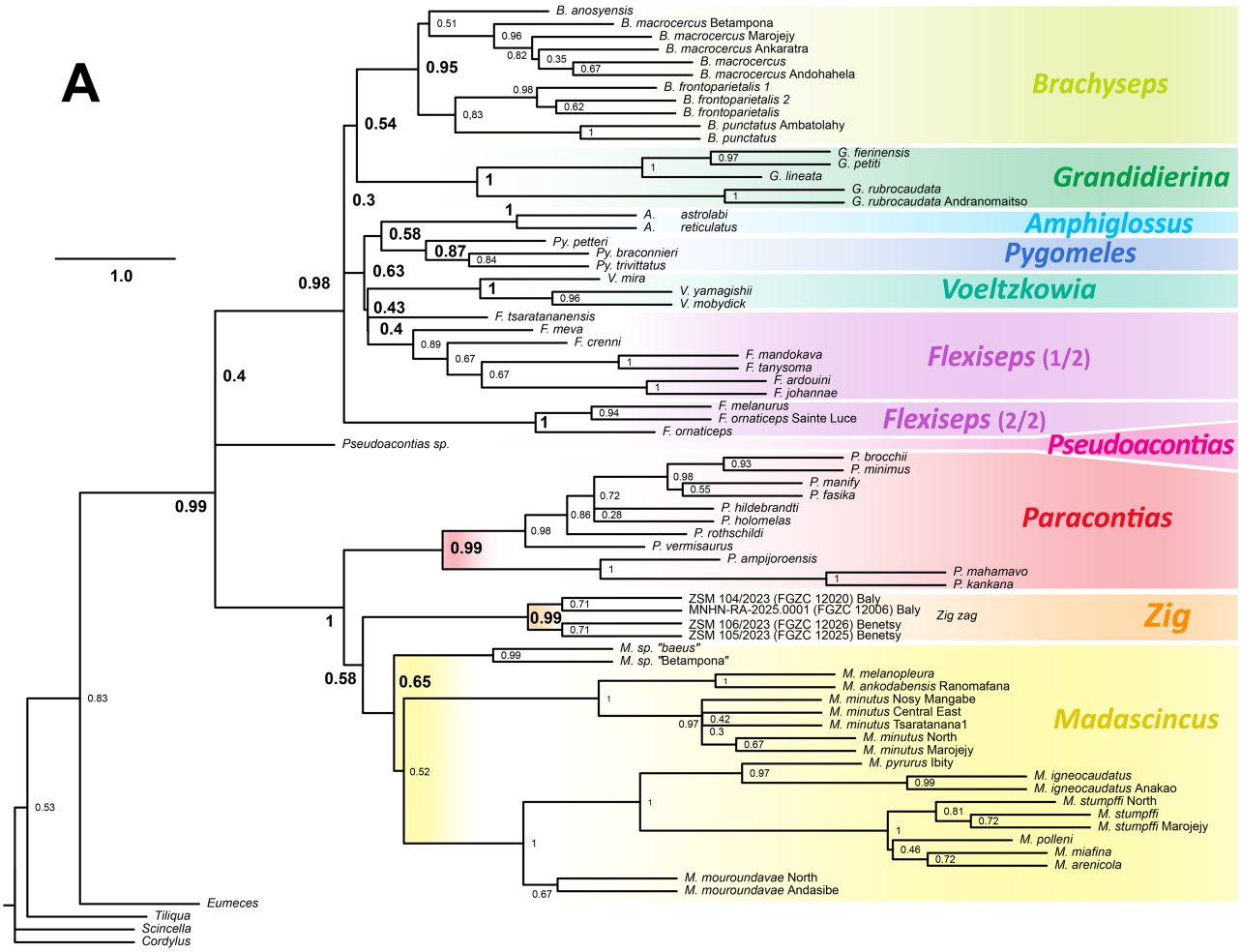

FIGURE 4. (A) Species tree reconstructed with ASTRAL (based on 11 gene trees from 10 nuclear gene fragments and concatenated mitochondrial sequences). (B) Comparison of the three distinct genus-level topologies estimated herein: (B1) Tree based on the RADseq dataset (Maximum likelihood approach), and trees inferred from the supermatrix of Sanger sequences based on a concatenated multilocus BI (B2) or ASTRAL species tree reconstruction (B3). Weak node support values (below 0.80) are represented in red. Despite several notable topological incongruencies, all analyses agree with strong support that *Zig zag* **gen. nov. & sp. nov.** is nested within the clade A, and that the three genera forming this clade (*Paracontias*, *Madascincus* and *Zig*) are reciprocally monophyletic.

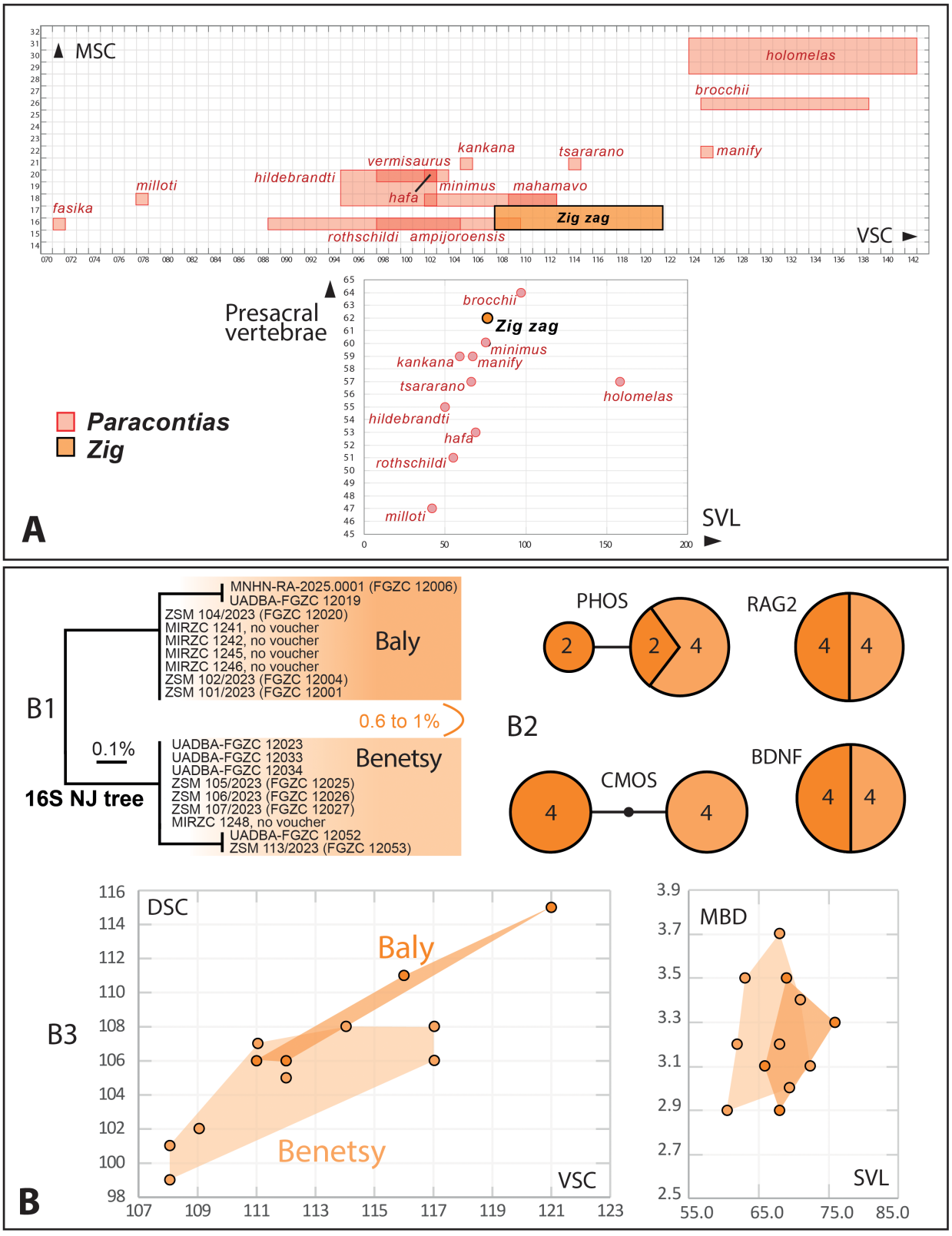

FIGURE 5. (A) Overview of the morphological divergence between *Zig zag* **gen. nov. & sp. nov.** and species of the genus *Paracontias* (i.e. members of the *ZiPa* clade). MSC: Mid-body scale counts, VSC: Ventral scale counts, SVL: snout vent length. The high number of ventral scales (counted longitudinally along the body) relative to the low number of scales around the body suggest that the body shape in *Zig* is relatively thinner and more elongated when compared to *Paracontias* species. (B) Intraspecific divergence between Baly and Benetsy populations of *Zig zag* **gen. nov. & sp. nov.**: (B1) Genetic divergence based on a NJ tree for 16S, (B2) haplotype genealogies reconstructed from fragments of the four nuclear-encoded genes PDC, RAG2, CMOS and BDNF, and (B3) morphological divergence based on dorsal scale counts (DSC) and ventral scale counts (VSC), and on mid-body diameter (MBD) and snout-vent length (SVL) in millimeters. Populations from Baie de Baly and from Benetsy highlighted in dark and light orange, respectively.

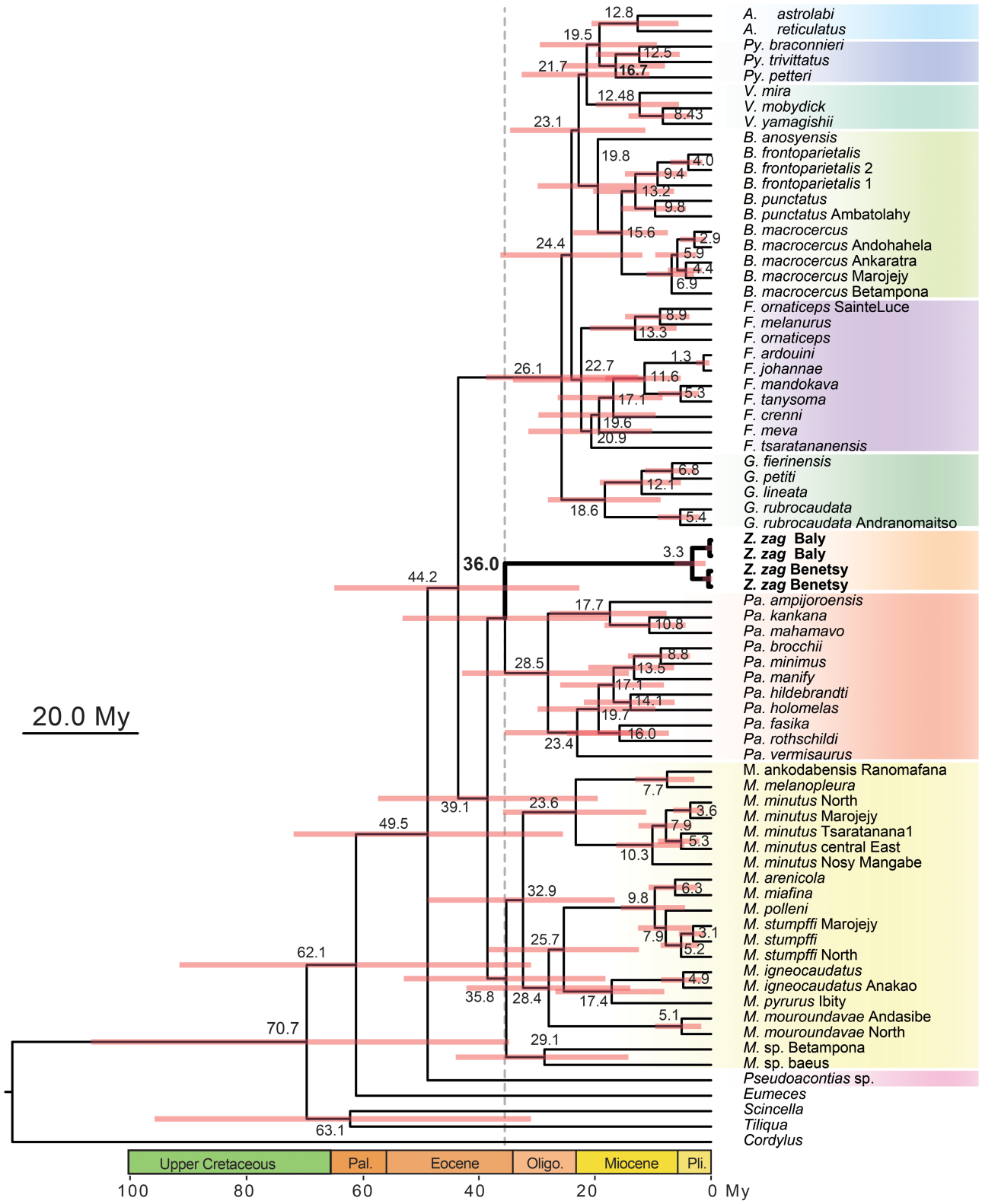

FIGURE 6. Divergence times estimated with BEAST on the concatenated multilocus matrix of the BI tree. Horizontal red segments are representing confidence intervals (time expressed in million years), and the vertical dashed line in grey is representing the split of the new genus *Zig*.

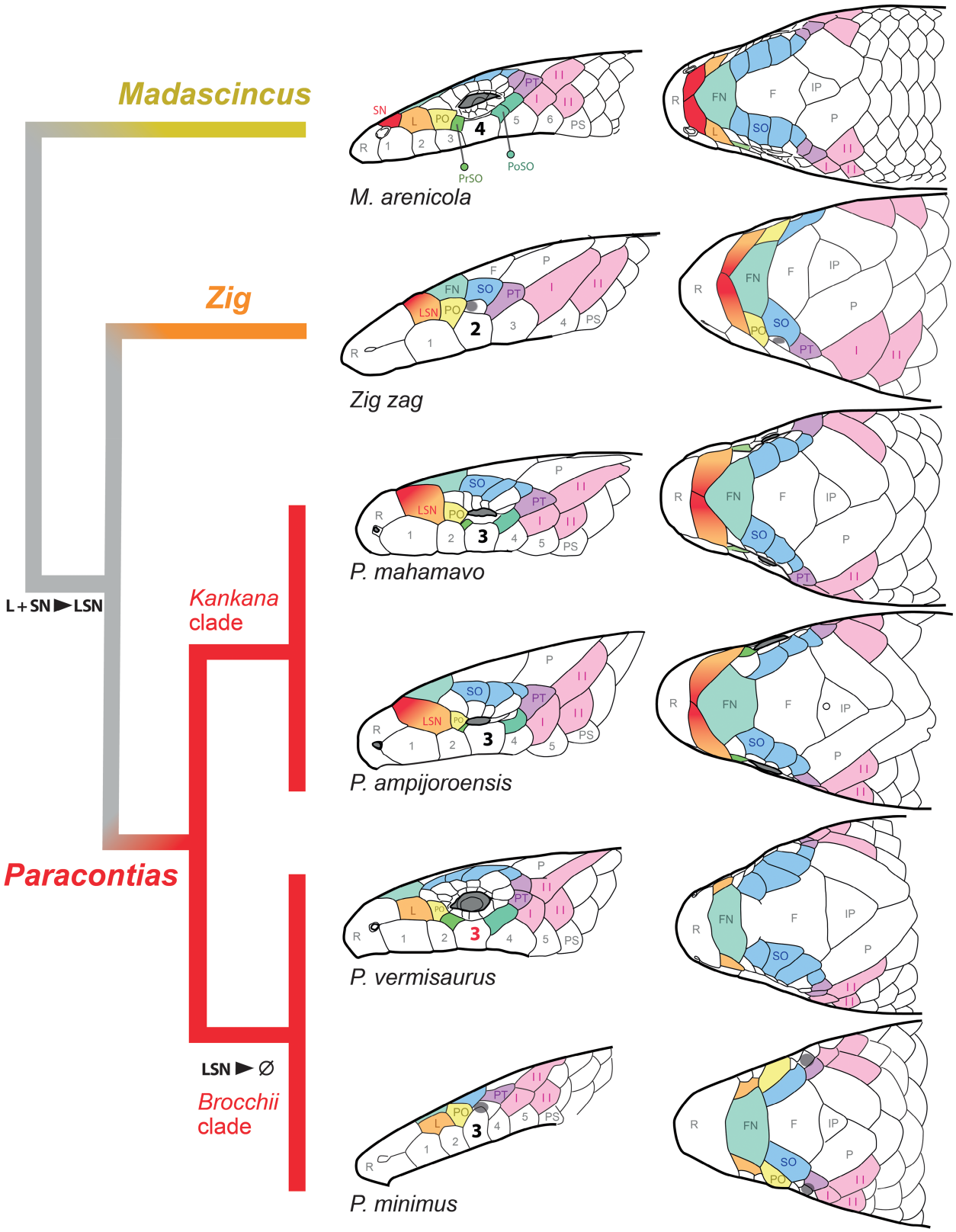

FIGURE 7. Comparison of cephalic scale patterns between *Zig* **gen. nov.** and its sister genus, *Paracontias* (i.e. *ZiPa* clade). For *Paracontias*, four species belonging to the two main clades within the genus were selected (i.e. *Brocchii* and *Kankana* clades, cf. Miralles *et al.* 2016a). One species of *Madascincus* (a quadruped and pentadactyl genus supposedly sister to the *Paracontias+Zig* clade) is included for comparison to illustrate the presumed plesiomorphic state of a more fragmented pattern of head scales. The scale terminology used refers to the presumed ancestral pattern of *Madascincus*: R: rostral / rostral shield, L: loreal, SN: supranasal, LSN: loreo-supranasal (i.e. L+SN), FN: frontonasal, F: frontal, SO: supraocular, IP: interparietal, P: parietal, PO: preocular, PrSO: presubocular, PoSO: postsubocular, PT: pretemporal, I, II: primary and secondary temporal, numbered 1 to 6: supralabials (subocular supralabial highlighted in bold).

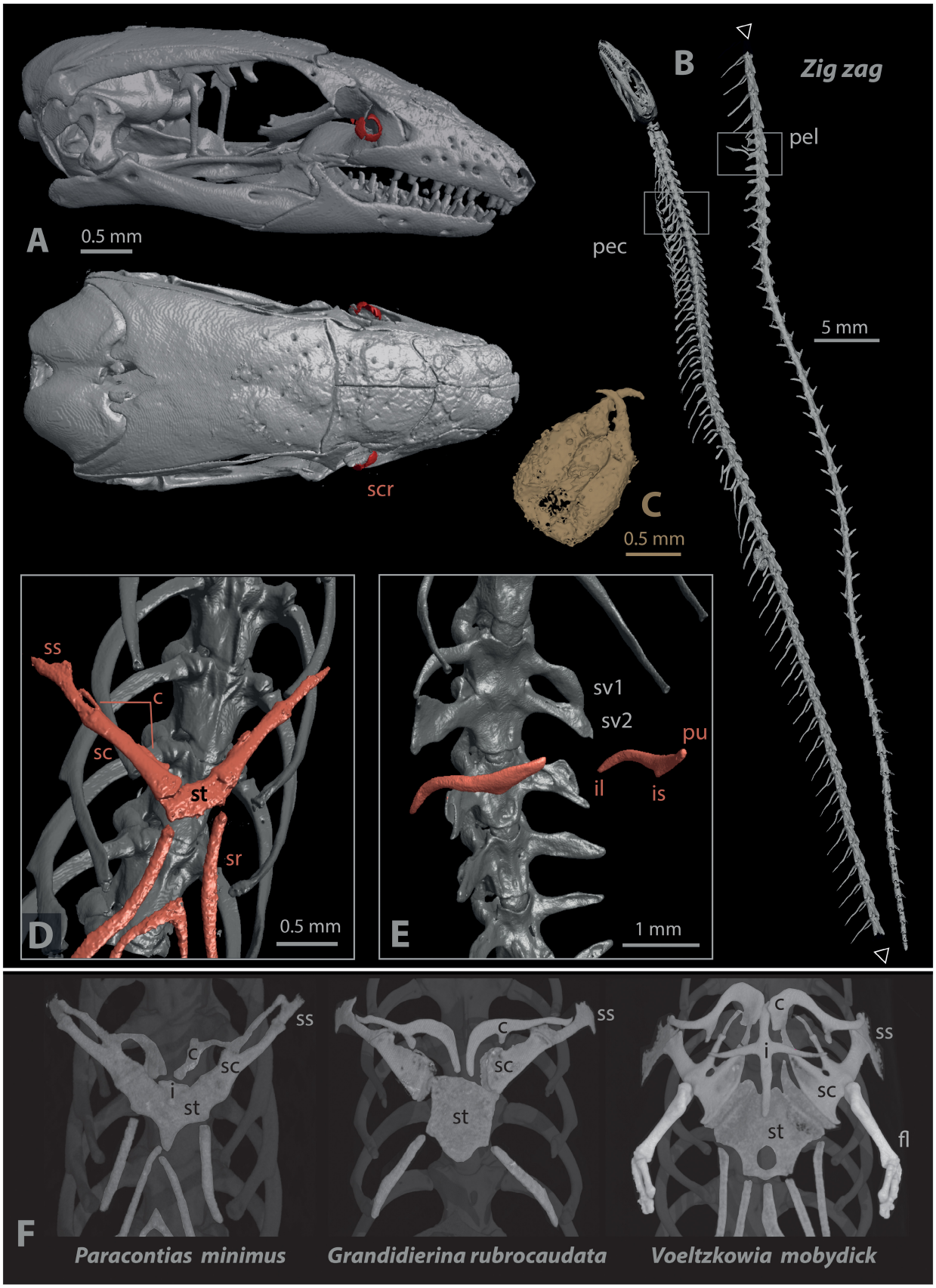

FIGURE 8. Micro-computed tomographic reconstruction of the skeleton of *Zig zag* **gen. nov. & sp. nov.** (Holotype MNHN-RA-2025.0001): (A) head, (B) whole specimen (picture cut in to part), (C) head of a termite revealed in the digestive tract, (D) pectoral and (E) pelvic girdle, (F) pectoral girdle of other Malagasy sand-fossorial limbless skinks (from Miralles *et al.* 2015). Legend: clavicle (c), interclavicle (i), pectoral (pec) and pelvic (pel) girdles, sternum (st), scapulocoracoid (sc), sclerotic ring (scr), suprascapulae (ss), sternal ribs (sr), residual forelimb elements (fl), sacral vertebrae (SV1 and (2), ilium (il), ischium (is), pubis (pu).

Divergence date estimation

Despite significant uncertainties, the estimated divergence times of Malagasy Scincinae (Fig. 6), consistent with the reconstruction of Belluardo *et al.* (2023), allow to tentatively place the divergence between *Paracontias* and the new taxon *Zig* **gen. nov.** into a temporal context. The most recent common ancestor of the group was dated in the middle Eocene, at 49.5 Ma (95% HPDI: 72.8–26.1 Ma) and the divergence between clade A and B at 44.2 Ma (95% HPDI: 65.6–23.2 Ma). According to our timetree, the split between the genus *Madascincus* and the clade composed of *Zig* **gen. nov.** and *Paracontias* (clade *ZiPa*) occurred at 39.1 Ma (95% HPDI: 58.0–20.0 Ma), while *Zig* **gen. nov.** diverged from *Paracontias* near the Eocene-Oligocene transition (~34 Ma), at 36.0 Ma (95% HPDI: 53.7–18.2 Ma).

Morphology and skeletal anatomy

Based on 16 specimens collected at two localities 55 km apart (four from Baie de Baly and eight from Benetsy), external morphological examination revealed a combination of several traits that unambiguously distinguishes *Zig zag* **gen. nov. & sp. nov.** from all other Malagasy scincine skinks. The main morphological discriminant traits are presented in the genus, and species diagnoses in the taxonomic section below. See also Fig. 5A and Fig. 7 for an overview of the main features differentiating *Zig* **gen. nov.** from its sister genus *Paracontias*.

The micro-CT results obtained from the holotype specimen MNHN-RA-2025.0001 are illustrated in Fig. 8 and detailed in the species description below. Compared to other fossorial Malagasy scincine species, such as members of the genus *Grandiderina*, *Voeltzkowia* and *Paracontias minimus* (cf. Miralles *et al.* 2015), *Zig zag* **gen. nov. & sp. nov.** shows a maximum level of scapular and pelvic girdle regression. In contrast to the aforementioned taxa, the pectoral girdle of *Zig* **gen. nov.** is very short (i.e. sternum clearly wider than long) and the clavicles are virtually absent (a few traces interpreted here as clavicle residues seem to be largely fused with the thin and cylindrical scapulocoracoid). Furthermore, tomography was not able to reveal the presence of any residual elements of the fore- or hind limb. Similarly, *Zig* **gen. nov.** shows a remarkable regression of the sclerotic ring, with only three ossicles per eye (to be compared with *Voeltzkowia mobydick*, which has 5 ossicles).

As in other Malagasy limbless fossorial scincines, *Zig* **gen. nov.** has undergone significant simplification by fusion of its cephalic scales (i.e., fewer but larger scales). Among the most striking changes are the drastic reduction in the number of scales in the ocular and periocular region (i.e. lidless eye without opening, completely covered by a single ocular scale) and the formation of an enlarged rostral shield covering a large part of the snout. Moreover, *Zig* **gen. nov.** shares with species of the *Kankana* clade (i.e. *P. kankana*, *P. ampijoroensis* and *P. mahamavo*) an unusual scale pattern on the loreal / nasal region: a pair of scales in contact with each other and with the rostral shield replaces both the supra-nasal scales (defined in other scincine species as the pairs of scales located dorsally between the rostral and the fronto-nasal) and the loreals (defined as the paired scales, present on each side of the snout, and framed anteriorly by the rostral, posteriorly by the pre-ocular, dorsally by the frontonasal and ventrally by the first supralbial). Consequently, it is not possible to define unambiguously whether these paired scales are homologous with supranasals or loreals (i.e. progressive regression of one type of scale in favor of the other, or vice versa) or with both (i.e. disappearance of the suture that distinguishes one from the other). For this reason, we interpret them pragmatically as a "combination" of the two and refer to them as loreo-supranasal.

Additionally, morphological polymorphism within and between both sampled populations of *Zig* **gen. nov.** has been assessed and is summarized in Table 2 and Fig. 5B3. These data show that both populations are overall very similar in terms of head scale configuration, body coloration, size, and scale counts. They only differ by (1) a slightly higher number of longitudinal scale rows along the body in the population from Baie de Baly (106–115 dorsals vs. 99–108 in Benetsy; and 111–121 ventrals vs. 108–117 in Benetsy), and (2) a slightly higher body length / body width ratio (SVL/MBD) in Baie de Baly specimens.

Evolution of substrate type preferences

The MP and ML ancestral states analyses for substrate preferences (*psammophilous* versus *humicolous* ecology) reconstructed very contrasting scenarios (Fig. 13B):

At first glance, the MP ancestral state reconstruction does not reveal a strong phylogenetic pattern, as both ecological preferences are distributed across the tree without a clear lineage-based trend. This approach inferred two alternative equally parsimonious scenarios, each requiring five evolutionary transitions. Any alternative reconstruction would require at least two additional steps, making them less likely under the maximum parsimony criterion. These two scenarios differ primarily in how they interpret the transitions within the *P. brocchii* clade. As a result, it remains unresolved whether the presence of psammophily within this subgroup represents a retained ancestral trait (i.e., involving four transitions from sand to humus habitats), or a case of multiple independent reversals to psammophily following a single shift to humicolous ecology. However, and more interestingly, both agree on an ancestral psammophilous condition at the root of the *ZiPa* clade (i.e. the two most basal nodes).

For the ML approach, the full HiSSE model incorporating two hidden states and allowing state-specific variation in speciation, extinction, and transition rates (while excluding dual transitions simultaneously changing both the observed and hidden states), was identified as the best-fitting model across all posterior trees based on AICc weights (Appendix 3). The ancestral state reconstruction performed on this model identified the ancestral state of the *ZiPa* clade as unequivocally humicolous, with the seven psammophilous species present in our dataset each representing a distinct and convergent transition from humus to sand habitats.

Taxonomy

Zig gen. nov.

urn:lsid:zoobank.org:act:468F53A8-A2AF-41C0-ADD7-4E68F3058614

Type species. Zig zag **sp. nov.** See the species description below.

Etymology. The name *Zig* is an arbitrary combination of letters in the sense of the International Code of Zoological Nomenclature Articles 30.1.4.1 and 30.2.2, and we assign it the feminine gender. We have searched all available taxonomic databases and could not find any evidence that this name has ever been used to refer to a genus of animals, and we therefore conclude that it is available.

Diagnosis of the genus Zig. Based on molecular phylogenetic relationships, a genus in the family Scincidae, subfamily Scincinae, sister to *Paracontias*. The genus *Zig* is distinguished from all other known Malagasy scincines by the following combination of characters: (1) the complete absence of limbs (versus four well developed and pentadactyl limbs in *Madascincus, Amphiglossus, Flexiseps, Brachyseps,* and relictual fore- and hindlimbs in some—but not all—species of *Grandidierina*, *Pygomeles, Pseudoacontias, Voeltzkowia*), (2) a "blind" morphotype (versus presence of an eye-opening, in *Amphiglossus, Flexiseps, Brachyseps, Madascincus, Pygomeles, Pseudoacontias,* and all *Paracontias* species except *P. minimus*), (3) the presence of a single supraocular (versus two to four supraoculars, most often four, in *Amphiglossus, Flexiseps, Brachyseps, Madascincus, Pygomeles, Pseudoacontias,* and all *Paracontias* species except *P. minimus*), (4) the absence of a visible external ear-opening (versus present and well distinguishable in *Amphiglossus, Brachyseps*, *Flexiseps* except *F. stylus*, and *Madascincus*), (5) the fusion of the supranasals and loreals into loreo-supranasals (a condition otherwise only encountered in the three known species forming the *Kankana* clade, i.e. *Paracontias kankana*, *P. ampijoroensis* and *P. mahamavo*), and two autapomorphic traits only found in *Zig*, i.e. (6) the presence of single, significantly enlarged secondary temporal, as elongated as the primary temporal and in contact with the last supralabial and the nuchal (versus presence of two secondary temporals in all the other genera), and (7) the position of the subocular scale corresponding to the second supralabial (versus the third, the fourth, or occasionally the fifth in all the other genera).

Distribution. Madagascar, Mahajanga basin, western bank of the Betsiboka River. See more details in the species description section below.

Zig zag sp. nov.

urn:lsid:zoobank.org:act:C7FED2DF-6AC3-4A5E-8B7E-15BC5E2598DC
(Figs 8–10)

Holotype. MNHN-RA-2025.0001 (formerly ZSM 103/2023, field number FGZC 12006), white sand area 3 km north of Village de Baly (16.048420° S, 45.271180° E, ca. 10 m a.s.l.), Baie de Baly National Park, Boeny region, Northwest of Madagascar, collected on 14 October 2023, between 05:00 and 06:30 a.m., by A. Miralles and N. A. Rahagalala.

Paratypes (25 specimens). ZSM 101/2023 (FGZC 12001), ZSM 102/2023 (FGZC 12004), UADBA-FGZC 12002, 12003, 12005, same collection data as the holotype. ZSM 104/2023 (FGZC 12020), UADBA-FGZC 12018, 12019, white sand area 2.5 km north to the Village de Baly (16.051937° S, 45.271192° E, ca. 10 m a.s.l.), Baie de Baly National Park, Boeny region, Northwest of Madagascar, collected on 14 October 2023, between 08:00 and 09:00 p.m. by A. Miralles and N. A. Rahagalala. ZSM 105/2023 (FGZC 12025), ZSM 106/2023 (FGZC 12026), ZSM 107/2023 (FGZC 12027), ZSM 108/2023 (FGZC 12028), ZSM 109/2023 (FGZC 12029), ZSM 110/2023 (FGZC 12030), ZSM 111/2023 (FGZC 12031), ZSM 112/2023 (FGZC 12032, juvenile), UADBA-FGZC 12021, 12022, 12023, 12024, 12033, 12034, 12035, white sand area 1 km South East to the village of Benetsy (15.939187° S, 45.770564° E, ca. 15 m a.s.l.), Tsiombikibo forest, Boeny region, North West of Madagascar, collected on 16 and 17 October 2023, between 08:00–09:30 p.m. and between 05:00–06:00 a.m. by A. Miralles and N. A. Rahagalala. ZSM 113/2023 (FGZC 12053), UADBA-FGZC 12052 (juvenile), white sand area 6 km East to the village of Benetsy (15.946133° S, 45.818431° E, ca. 20 m a.s.l.), Tsiombikibo forest, Boeny region, Northwest of Madagascar, collected on 18 October 2023, between 09:00 and 09:30 a.m. by A. Miralles and N. A. Rahagalala.

Additional material. Based on photographic examination of two specimens (UMMZ 238174, 238178, G. Schneider pers. comm., Fig. 9E), twenty-three specimens deposited at the UMMZ (all registered as *Voeltzkowia* sp.) can in all likelihood be assigned to *Zig zag*: UMMZ 238171–238191, village of Antsakoamanery (16°1.270'S, 45°36.174'E), near Tsiombikibo forest, Boeny region, Northwest of Madagascar), collected between 15 and 21 March 2002 by J. Spannring, J. Rafanomazatsoa and M. Rakotoarivelo. UMMZ 238192, 238193, village of Benetsy (15°55.952'S, 45°46.294'E), near Tsiombikibo forest, Boeny region, Northwest of Madagascar), collected on 28 March 2002 by J. Spannring, J. Rafanomazatsoa and M. Rakotoarivelo.

Etymology. The specific epithet '*zag*', an arbitrary combination of letters, is used here to form a pun on 'zig zag', in reference to the very characteristic sinusoidal tracks left by this species when moving in the white sand. It is treated as an invariable noun in apposition to the genus name.

Diagnosis. As *Zig* represents a monotypic genus, the generic diagnosis of *Zig* above is also suitable to distinguish the species *Zig zag* from any other Malagasy scincine species. Additionally, *Zig zag* differs from the other superficially similar worm-like Malagasy species (i.e. limbless, "blind", elongated and miniaturized morphotype such as *Grandidierina* spp., *Voeltzkowia* spp. and *Paracontias minimus*) by the following combination

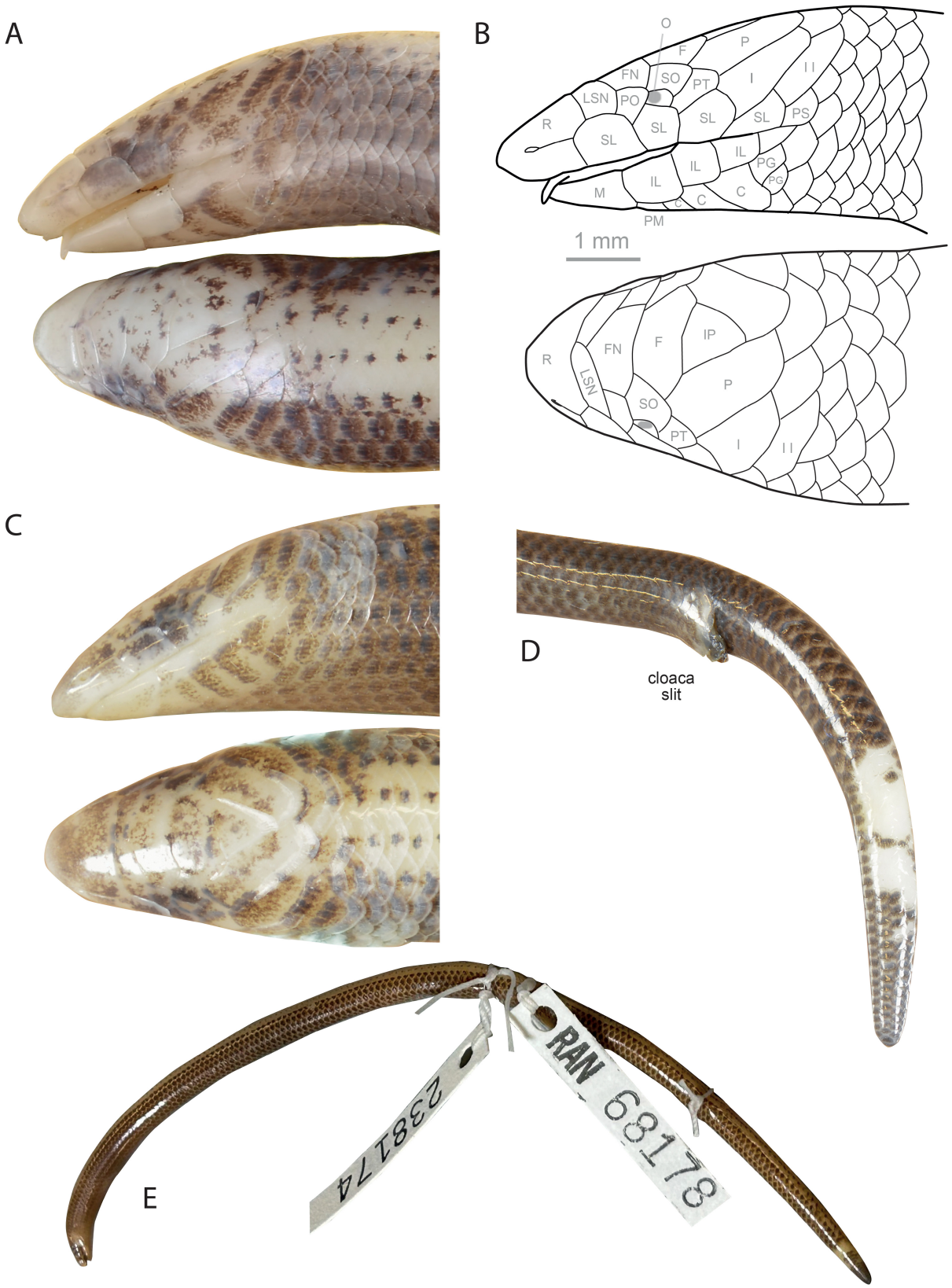

FIGURE 9. Preserved specimens of *Zig zag* **gen. nov. & sp. nov.** from three distinct localities. Detail of the head in lateral and dorsal views of (A) the holotype MNHN-RA-2025.0001, from Baie de Baly, with (B) the corresponding head scale pattern drawn with respective interpretation (dorsal view mirror-reversed), and (C) of the paratype ZSM 106/2023, from Benetsy, with (D) a lateral view of its tail, showing a wide white patch of totally discolored scales. (E) Specimen UMMZ 238174 from Antsakoamanery in lateral view. Head scale abbreviations: C: chin shield, F: frontal, FN: frontonasal, IL: infralabial, IP: interparietal, LSN: loreo-supranasal, M: mental, O: ocular, P: parietal, PG: post-genial, PO: preocular, PT: pretemporal, PS: post-supralabial, R: rostral shield, SL: supralabial, SO: supraocular, I and II: primary and secondary temporal. Photographic images not not to scale.

FIGURE 10. Coloration in life of *Zig zag* **gen. nov. & sp. nov**: Holotype MNHN-RA-2025.0001 and paratype ZSM 104/2023 in dorsolateral and lateral views, both from Baie de Baly; and paratypes ZSM 105/2023, ZSM 107/2023 (close-up of the dorsal, lateral and ventral view of the head), ZSM 108/2023 and ZSM 112/2023 (juvenile), all four from Benetsy. Not to scale.

of character states: (1) presence of paired loreo-supranasals in median contact, extending laterally until contacting supralabials (versus distinct supranasals and loreals in all species of *Grandidierina* and *Voeltzkowia*, and absence of supranasals and loreals (or loreo-supranasals) in *Paracontias minimus*); (2) complete absence of limbs (presence of relictual forelimbs in *Voeltzkowia yamagishii*, *V. mobydick* and *V. shaihulud*, and of relictual hindlimbs in *Grandidierina fierinensis* and *G. petiti*); (3) dark pigmented ventral side, highly contrasting with the light dorsal side (light or paler ventral side in *Grandidierina*, *Voeltzkowia* and *Paracontias minimus*); (4) presence of a rostral shield, i.e. absence of nasal scale, with the nostril deeply embedded within the rostral scale and posteriorly connected to the first supralabial by an horizontal groove (versus presence of a wedge-shaped nasal interlocking with the rostral, in *Grandidierina* and *Voeltzkowia*); and (5) a low number of scales (16–17) around midbody (versus 18–22 in *Grandidierina*, 18 in *P. minimus*, 18–20 in *Voeltzkowia*).

Description of the holotype. External morphology. (Figs 8–10). Unsexed specimen in a relatively good state of preservation, except for a small piece of skin (5 mm long and 2 mm wide) removed on the left side of the body and used as tissue sample, and the presence of a short dorsal incision at mid-body (Fig. 10). Snout-vent length 76.0 mm, tail length 52.0 mm, width at midbody 3.3 mm, head width at level of parietal scale 2.3 mm. In general, a very elongated and slender, limbless and small-sized, bicolored skink. Snout rounded in dorsal view, bluntly wedge-shaped in lateral view; rostral extends posteriorly dorsally; paired loreo-supranasals contacting medially and in broad contact laterally with the first supralabials; frontonasal pentagonal, two times wider than long; frontal hexagonal, two times wider than long; interparietal triangular, contacting frontal; parietals meet posterior to interparietal; enlarged nuchals absent; nasal absent, nostril deeply embedded within the rostral, posteriorly connected to the first supralabial by an horizontal groove (i.e. "Rostral shield" pattern sensu Miralles *et al.* 2011, 2015); preocular single, as longer as high, in contact with and extending between first and second supralabials, and also in contact with loreo-supranasal, frontonasal, supraocular and ocular; presubocular and postsubocular absent, likely fused together to form the ocular; supraocular single; ocular single, small, rectangular; eye sunken deeply below ocular, and the second supralabial; primary and secondary temporal single, extending dorsally and two times wider than long; supralabials four, the second in subocular position; external ear opening absent or not visible. Upper jaw distinctly projecting lower jaw; mental wider than long; postmental wider than long; infralabials three, first only in contact with postmental; three pairs of large chin scales, members of first and second pair separated by one scale row, members of third pair separated by three scale rows. Longitudinal scale rows at midbody 16; paravertebral scales 115 (including nuchals), similar in size to adjacent scales; ventral scales 121 (including postmental); four preanals. No external limbs visible, no traces indicating the ancestral position of the pectoral or pelvic girdles.

Osteology (Fig. 8). Sixty-two presacral vertebrae, two sacral vertebrae, and around 44 caudal (post-sacral) vertebrae (terminal one hardly distinguishable). Pectoral girdle is highly regressed, dorso-ventrally flattened, more than two times wider than long (2.2 × 1.1 mm), and chevron-shaped. Clavicles, extremely regressed and almost indistinguishable at their midlength, are apparently almost entirely fused to the scapulocoracoid. The interclavicle is absent or not visible. Suprascapulae are highly regressed, roughly rectangular, in continuity with the longitudinal axis of the scapulocoracoid bone axis. Scapula, coracoid and precoracoid cannot be distinguished from each other, forming a very regressed and compact cylindrical scapulocoracoid bone without foramina nor fenestra. The rectangular sternum, without a visible median fontanel, is two to three times larger than long, and in contact posteriorly with one pair of sternal ribs. Absence of xiphisternum. Eight pairs of poststernal ribs articulated medially with each other, forming continuous chevrons. Forelimbs are apparently completely regressed, with no visible vestigial bones. The pelvic girdle is highly reduced, composed of two separate elongated and curved hemipelves, without visible acetabular depression (1.6 × 0.14 mm). Pubis and ischium area are ventro-laterally flattened, whereas the ilium area forms an elongated cigar-shaped dorso-caudal projection. Hindlimbs are apparently completely regressed, with no visible vestigial bones. For both eyes, sclerotic rings are formed by only three visible ossicles.

Coloration (Figs 9, 10). After eight months in preservative, the body of the holotype is bicolored, with a light cream dorsal side and a brown latero-ventral side, with the width of the light dorsal side corresponding to that of 5 transverse rows of scales (mediodorsally, 4 rows of fully light scales, and on each side, dorsolaterally, one scale row whose scales are light only in their upper half). Each of the fully light scales exhibit a single distinct black dot in their center, giving the overall impression that four dotted black lines run longitudinally on the dorsum. Width of the dark latero-ventral side corresponding to that of 11 transverse rows of scales (medioventrally, 10 rows of fully dark scales, and on each side, dorsolaterally, one scale row whose scales are dark only on the lower half). The posterior margin of the dark scales is light cream. The ocular area is significantly darker than the rest of the head, and the rostal, mental and infralabial areas are immaculate light cream. Four scattered scales on the ventral side of the tail are entirely unpigmented. In life (Fig. 10), the coloration was overall similar, although brighter. The light dorsal side was beige-gold, and the dark ventral side was darker, almost black. The ocular region was darker than the rest of head, whereas the temporal and gular areas were slightly pinkish due to the active blood vascularization visible through the thin skin.

Variation. All specimens examined are rather similar to the holotype. The morphological variation of the holotype and 12 paratypes is presented in Table 2 and the variation of 12 adult specimens shown in Fig. 5B3. Color variation is shown in Fig. 10. At both localities, several specimens show wide, variable, irregular and elongated pure white flecks or blotches on the ventral—sometimes

TABLE 2. Intraspecific morphological variation within *Zig zag* **gen. nov. & sp. nov.** (HT: holotype, PT: paratypes). SVL: Snout-vent length, MBD: mid-body diameter, TL: tail length (tails regenerated, broken into several parts, or partly missing are marked with an asterisk), SL: number of supralabials (position of the subocular SL indicated between parentheses), VSC: ventral scale counts, DSC: dorsal scale counts, MSC: mid-body scale counts, ET: enlarged temporals, Nuch II: number of secondary enlarged nuchal scales. Bilateral traits are separated by a slash (right / left side, respectively).

Specimens	SVL (mm)	MBD (mm)	TL (mm)	SL	VSC	DSC	MSC	ET	Nuch II
Baie de Baly									
MNHN-RA-2025.0001 (HT)	76.0	3.3	52.0	4(2)/4(2)	121	115	16	3/3	0/0
ZSM 101/2023 (PT)	69.0	3.5	46.5	4(2)/4(2)	116	111	17	3/3	0/0
ZSM 102/2023 (PT)	68.0	2.9	22.0*	4(2)/4(2)	111	106	16	3/3	0/0
ZSM 104/2023 (PT)	66.0	3.1	42.5	4(2)/4(2)	112	106	16	3/3	0/0
Benetsy									
ZSM 105/2023 (PT)	62.0	3.2	36.0*	4(2)/4(2)	111	107	16	4/3	0/0
ZSM 106/2023 (PT)	72.5	3.1	18.0*	3(1)/4(2)	117	108	17	3/2	0/0
ZSM 107/2023 (PT)	68.0	3.2	32.0*	4(2)/4(2)	108	101	16	4/3	0/0
ZSM 108/2023 (PT)	63.1	3.5	18.0*	4(2)/4(2)	108	99	17	3/3	0/0
ZSM 109/2023 (PT)	69.5	3.0	50.9*	4(2)/4(2)	109	102	17	2/4	0/0
ZSM 110/2023 (PT)	68.0	3.7	16.9*	4(2)/4(2)	114	108	16	3/3	0/0
ZSM 111/2023 (PT)	60.5	2.9	34.0*	4(2)/4(2)	117	106	16	2/2	0/0
ZSM 112/2023, juv. (PT)	27.0	2.0	N/A*	4(2)/4(2)	N/A	N/A	16	3/2	0/0
ZSM 113/2023 (PT)	71.0	3.4	10.9*	4(2)/4(2)	112	105	16	2/3	0/0

ventrolateral—side of the tail (e.g., ZSM 105/2023, 106/2023, 107/2023, 108/2023, 111/2023,—see example in Fig. 9). This trait is apparently not correlated with whether the tail is regenerated or not.

Distribution. Zig zag **sp. nov.** is known from several white sand areas in the western side of the Mahajanga basin (west bank of the Bombetoka bay), specifically in Baie de Baly National Park, and in the Tsiombikibo forest near the village of Benetsy (north-eastern periphery of the forest) and possibly near the village of Antsakoamanery (western periphery of the forest) (Fig. 1). *Zig zag* is also likely present in the coastal area joining these two regions which are 55 km apart, as the Marambitsy Bay area and the complex Mahavavy Kinkony (CMK) protected area include many suitable habitats (white sand patches visible on satellite views). Eastwards from the known range, it is possible that the Mahavavy river delta represents a biogeographic barrier for the species, as we have not been able to find any sign of the presence of sand swimmer skinks during brief prospection in white sand areas of the Antrema protected area and at Katsepy. However, its presence in low densities cannot be ruled out here. Westwards, the species is likely present in the extended white sand areas located on the western coast of the Amparafaka cape (west of Baie de Baly National Park, unexplored in the present work). It might possibly extend further westwards to Cap Saint-André (Tanjona Vilanandro), unless the estuarine mangroves of the Antalihy (Antaly) bay represent a barrier too. The coast of Cape Saint-André indeed has several extended clusters of white sand areas, which, based on satellite images, are similar to those visited in Baie de Baly (approx. 60 km^2 of sparsely vegetated savannah on white sand, with apparently many palm trees).

Natural history and habitat. Like other sand-swimmer skinks from Madagascar, *Zig zag* **sp. nov.** probably spends most of its life buried in the sandy substrate and in leaf litter, in search of cool temperatures and shelter (Fig. 11, 12). At both known localities (Baie de Baly and Benetsy), the substrate is relatively similar, predominantly composed of almost pure quartz, coarse to medium, white sand (cf. details in Miralles *et al.* 2025).

During our field work, which took place in the dry season (October), all collected specimens were found in white sand savannah, in the shade of shrubs or trees. They were buried relatively deep in the sandy layer usually beneath a dense, 5–10 cm thick mat of fine roots, itself covered by a layer of dead vegetal matter and leaf litter of several cm thickness. Specifically, at Village de Baly, specimens were unearthed in the shade of large *Bismarckia* palm trees (>6 m height) growing in the middle of the white sand area, where the large debris of dead palms provided a supplementary protection from the sun (i.e. heat, light, evaporation). At Benetsy, specimens were found in the shade of 1–3 m high small leaf shrubs and bush clusters scattered over the white sand area. At both locations, numerous zig-zag tracks, similar to those left by species of *Grandidierina* or *Voeltzkowia*—but visibly narrower and less regular—were observed in the ungrown white sand surface and most likely were produced by this

FIGURE 11. Habitat of *Zig zag* **gen. nov. & sp. nov**. (A) White-sand savannah with *Bismarckia* palm trees near the village de Baly. (B) Shrubby white-sand savannah near the village of Benetsy. (C) Soil stratification in *Zig zag* microhabitat at Benetsy: (1) vegetation patches providing shade, (2) layer of dry vegetal litter, (3) dense mat of fine roots, (4) deeper layer made of almost pure white sand.

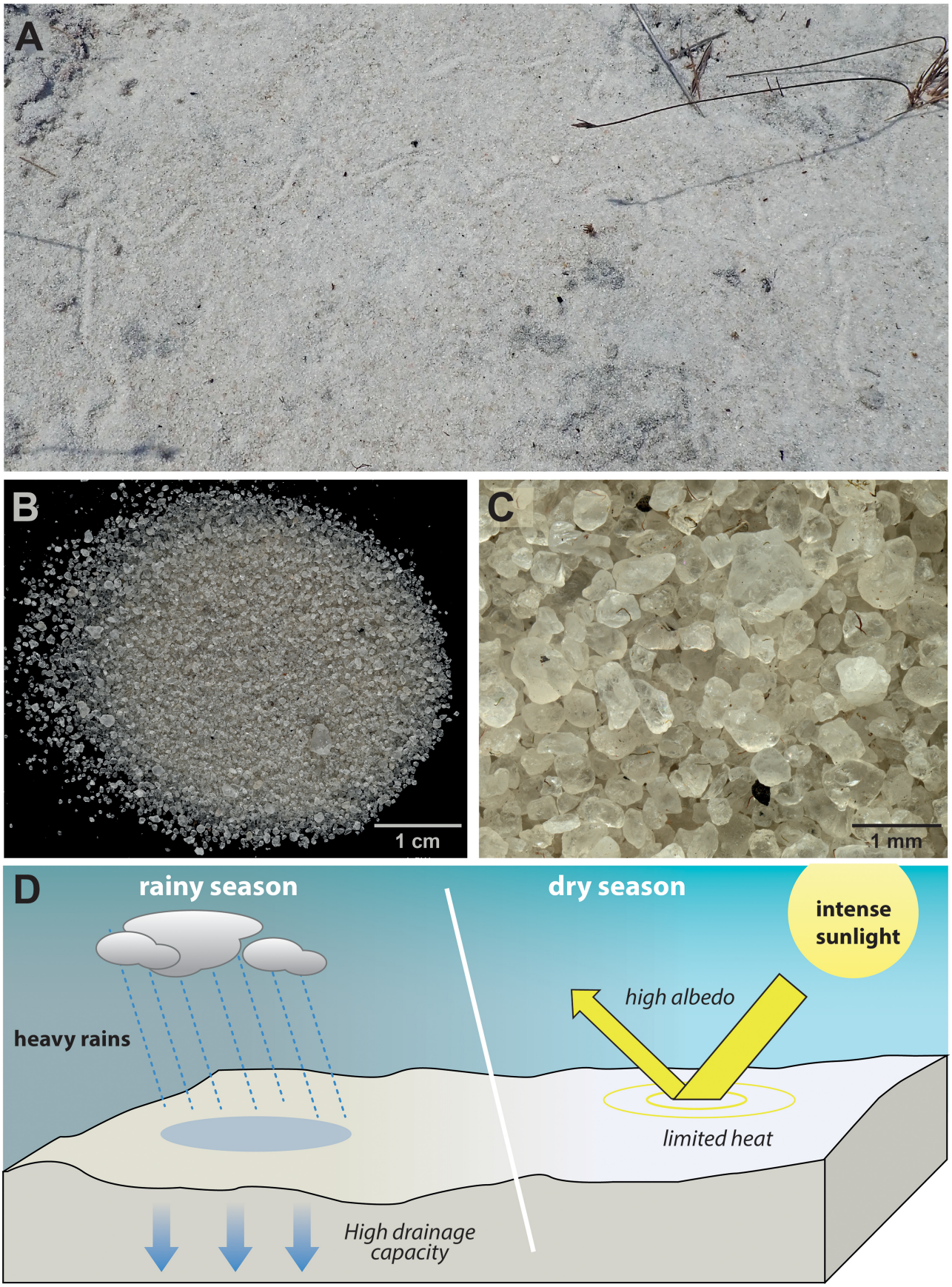

FIGURE 12. White sand substrate in *Zig zag* **gen. nov. & sp. nov.** habitats: In situ view of sand soil surface, with sigmoidal tracks let by *Zig zag* in Baie de Baly (A), and detailed views (B, C) of the almost pure quartz sand present in Benetsy (identical in Baly, see Miralles *et al.* 2025). (D) Diagram illustrating the physical properties of white sands when exposed to heavy rainfall or, conversely, to intense solar radiation. Photographs B and C by André Freiwald.

species. These tracks were probably left during nocturnal or twilight exploration of the surrounding area, when the sand has cooler temperatures than during the day. The abundance of these tracks suggests rather high local population densities.

Tomographic examination of the holotype revealed the presence of seven cephalic capsules of termites (Isoptera) with distinctly visible mandibles (Fig. 8C) in the digestive tract. As numerous columns of active termites were observed at night across the expanses of white sand at Baie de Baly, these insects might possibly represent a significant food resource for *Zig zag* **sp. nov.**, as has been shown for other limbless lizards living in arid sandy areas (e.g., *Typhlosaurus* in the Kalahari: Huey *et al.* 1974).

Conservation status. Based on the analysis of satellite imagery, the *extent of occurrence* (EOO) of *Zig zag* is estimated to be approximately 100 km², with a possible range between 80 and 120 km². This estimation is derived by summing the surface area of various white sand habitats located between Antaly Bay and Boina Bay. Consequently, the species' EOO is well below the IUCN Criterion B1 threshold of 5,000 km², and may even fall below the 100 km² threshold. The species' habitat is highly fragmented (IUCN Criterion B1-a), as the white sand areas are patchily distributed along the coastline and interrupted by deltaic rivers and estuarine mangroves. Due to this fragmentation, it is currently not feasible to provide a reliable estimate of the species' true area of distribution. Additionally, a continuing decline in both the *quality* and *extent* of suitable habitat is anticipated (IUCN Criterion B1-b). This is exemplified by the large-scale forest fire in 2022, which destroyed approximately 8,000 hectares of forest within Baie de Baly National Park (figure officially reported in multiple media by Madagascar National Parks). Assuming that the species may be distributed throughout its estimated EOO (which remains well below 5,000 km²) and taking into account the evidence of severe fragmentation and projected habitat decline (Criteria B1-a and B1-b), we recommend classifying *Zig zag* **sp. nov**. as Endangered (EN) under IUCN Red List Category B1 (IUCN Standards and Petitions Committee 2024).

Discussion

Justification for a new genus

Genus-level classification should rely on sound biological grounds and contribute to tailor size-manageable supraspecific categories, while preserving as much as possible nomenclatural stability so as not to compromise our future ability to communicate universally on biodiversity (Vences *et al.* 2013). The concept of *Zig* as a new genus is justified by its significant genetic and morphological differentiation from all other major scincine lineages, and by its phylogenetic position. Our nomenclatural decision is compliant with all the taxon naming criteria (TNC) of primary importance recommended by Vences *et al.* (2013) to prevent unnecessary taxonomic inflation at a supraspecific level (see Mahony *et al.* 2024), namely: (i) the genus *Zig* represents a newly discovered phylogenetic lineage distinct from all other recognized genera (i.e. not nested within them), and its erection does not disrupt the nomenclatural stability of Malagasy scincines (i.e., parsimony of taxonomic change; Scherz *et al.* 2017). The definitions of all the other genera remain indeed unchanged, as they all remain monophyletic and retain exactly the same composition in described species; (ii) the reciprocal monophyly between *Zig* and its sister genus, *Paracontias*, is very robustly supported by two largely independent molecular datasets (multi-locus Sanger data-set and RADseq); (iii) *Zig* is morphologically unambiguously distinguishable from all other Malagasy scincine genera by a series of diagnostic traits which include two strict autapomorphies (derived character states not found in any other species) which consist in (1) the presence of single, significantly enlarged secondary temporal and (2) the position of the subocular scale which correspond to the second supralabial. Additionally, although this morphological trait is not perfectly discriminating, *Zig* also differs from *Paracontias* by a lower number of mid-body scale counts (MSC) compared to the number of dorsal scale counts (DSC), and a high number of presacral vertebrae relative to the snout-vent length, suggesting a more elongated and narrow body shape (Fig. 5A). Finally, (iv) the phylogenetic trees reconstruct the taxon on a long and ancient branch (among the third or fourth oldest branch over 10 genus-level branches, and likely dating to the Eocene-Oligocene transition), thereby identifying it as one of the most divergent lineages within the scincine radiation in Madagascar.

A monotypic genus? Integrative assessment of Zig intrageneric divergence

Because both the RADseq and multilocus Sanger sequence datasets clearly support the monophyly of the two populations of *Zig* sampled (from Baie de Baly and from Benetsy), we assessed molecular and morphological data to explore whether the differentiation between the two populations, located 55 km apart, might be indicative of a potential signal of species-level differentiation.

Complementary analyses involving a larger number of samples (n=18) for the 16S mitochondrial DNA fragment revealed relatively low uncorrected *p*-distances between both populations (0.6–1%). In other genera of Malagasy scincines, such values for 16S clearly correspond to infraspecific levels of divergence (*Madascincus*: Miralles *et al.* 2011c; Miralles & Vences 2013; *Flexiseps* and *Amphiglossus*: Miralles *et al.* 2011a; *Paracontias*: Miralles *et al.* 2011b, 2016a; *Voeltzkowia* and *Grandidierina*: Miralles *et al.* 2025). Additionally, the four haplotype networks reconstructed from nuclear loci show a very low overall allelic diversity, with only two different haplotypes for PDC and CMOS, and a unique common haplotype for BDNF and for RAG2. From a morphological perspective, both populations are overall very similar in terms of head scale configuration, body coloration, size, and scale counts, and only differ by slightly different numbers of longitudinal scale rows along the body and body length / body width ratio. Both traits suggest that the Baie de Baly population might present a slenderer body shape

than the Benetsy population, a tendency also indicated by photographs (Fig. 5B3). However, neither of these two traits, widely overlapping, unambiguously discriminates between the two populations. Taken together, the low uncorrected *p*-distance in the mitochondrial 16S sequences, the weak differentiation in nuclear-encoded genes, and the absence of any unambiguous diagnostic morphological trait prompt us to consider the populations from Baie de Baly and Benetsy as belonging to the same biological species, *Zig zag*.

Evolutionary origin of the Zig-Paracontias clade
The most ancient lineage of Malagasy legless fossorial skinks?

Zig and *Paracontias* are recovered as forming a monophyletic group (here coined *ZiPa* clade) based on the analysis of concatenated Sanger-sequenced loci and of the RADseq dataset. This hypothesis is also supported by the presence of a derived morphological feature only present in *Zig* and in all species of the *Kankana* clade (i.e. absent in all other Malagasy scincines): the presence of loreals and supranasals fused into larger loreo-supranasal scales, in all likelihood, correspond to a transitional state between a plesiomorphic scaling pattern (where supranasals and loreals are both present and distinct from each other, a trait widely distributed among most Malagasy scincines) and a more derived one (complete absence of supranasals and loreals) present in all species of the *Brocchii* clade (See Appendix 5, and Miralles *et al.* 2016a). Based on parsimony considerations, it can be deduced that the evolutionary transition toward an apodal body form most likely occurred only once in the *ZiPa* clade, prior to its last common ancestor.

Based on the time tree, the *ZiPa* clade dates to the late Eocene (divergence from *Madascincus* estimated at 39 Ma, and divergence between *Zig* and *Paracontias* around 36 Ma) and would then be more than twice as old as other Malagasy sand-fossorial genera, which date back to the mid-Miocene (Miralles *et al.* 2025). The very pronounced regression of the pectoral and pelvic girdles in *Zig* and *Paracontias* (far more extreme than in *Voeltzkowia* and *Grandidierina*), the absence of any visible residual limb elements (which are still present in *Voeltzkowia*, *Grandidierina*, and *Pseudoacontias*) and the remarkably lower number of sclerotic ossicles in the eyes (three in *Zig zag*, five in *Voeltzkowia mobydick*), add additional support to the hypothesis that limb loss / fossoriality in the *ZiPa* clade occurred earlier than in the other limbless Malagasy lineages (*cf.* Miralles *et al.* 2015). Thus, unlike *Grandidierina*, *Voeltzkowia* and *Pygomeles*, and despite dating uncertainties, a mid-Miocene emergence of the limbless *ZiPa* clade can be reasonably excluded.

A high species diversity in the North, but a likely origin in the Northwest.

Until relatively recently, species forming the genus *Paracontias* were mainly known from northern Madagascar (as defined by Brown *et al.* 2016: i.e., roughly delimited by a diagonal spanning from 15.5°S on the east coast to ca. 15.0°S on the west coast), with the exception of only one species, *P. holomelas*, whose range extends further southwards along the eastern coast of the island. This suggested that the origin and center of diversification of these skinks is located in northern Madagascar, a common biogeographic pattern observed in various clades of the island's herpetofauna, for instance in frogs of the subfamily Cophylinae and of the mantellid genus *Gephyromantis* (Wollenberg *et al.* 2008; Kaffenberger *et al.* 2012). The relatively recent discoveries of the three species forming the *Kankana* clade (i.e. *P. kankana* described by Köhler *et al.* 2009, and *P. mahamavo* and *P. ampijoroensis*, both by Miralles *et al.* 2016b), have however tempered this hypothesis, since all of them are found at more southern sites, specifically in the Central Eastern region and the Mahajanga basin, respectively. The present discovery of *Zig* in the south-western part of the Mahajanaga basin further contradicts the hypothesis of a far northern origin of *Paracontias* (Fig. 13A). Based on the phylogenetic estimates, the *ZiPa* clade might have originated in the region of the Mahajanga basin and then dispersed toward northern Madagascar where later the *Brocchii* clade diversified. *Zig* and two of the three *Paracontias* species of the *Kankana* clade are indeed endemic to WS areas encircling the Mahajanga basin. Specifically, *Zig* and *P. mahamavo* occur in coastal WS areas located on the West and East of the Betsiboka delta, respectively, whereas *P. ampijoroensis* is found in the inland WS area of the Ankarafantsika National Park.

Origin of sand-fossoriality within the ZiPa clade.

All species within the *ZiPa* clade are fossorial skinks that inhabit the uppermost soil layers. Although detailed ecological data are scarce, field observations and specimen records indicate that each of these soil specialist species show strong preferences for one of two specific substrate types, with little overlap or intermediate preferences. Two ecological groups can therefore be distinguished: psammophilous species, which favor sandy substrates, and humicolous species, which prefer humus-rich, usually moist, organic soils. Placing the evolution of these traits within a chronological framework (i.e., a time-calibrated phylogenetic tree) not only enhances our understanding of the evolutionary origins of these fossorial organisms but may also provide valuable insights into the paleoclimatic history of Madagascar. The two approaches involved to reconstruct habitat preferences ancestral state (maximum parsimony, MP, and maximum likelihood, ML) produced substantially divergent outcomes, resulting in two distinct scenarios, both plausible though opposed, for the evolutionary origin of sand fossoriality in this group:

(1) Recent origins hypothesis. The ML approach supports a humicolous ancestral condition for the *ZiPa* clade, with each of the seven psammophilous species corresponding to distinct and repeated transitions from humus to sand habitat. In the absence of derived traits shared by at least two species, it is therefore challenging to position this transformation in a temporal frame. At best, the dates of divergences between psammophilous and humicolous sister species suggest that all these recurrent adaptations to sandy substrates occurred relatively

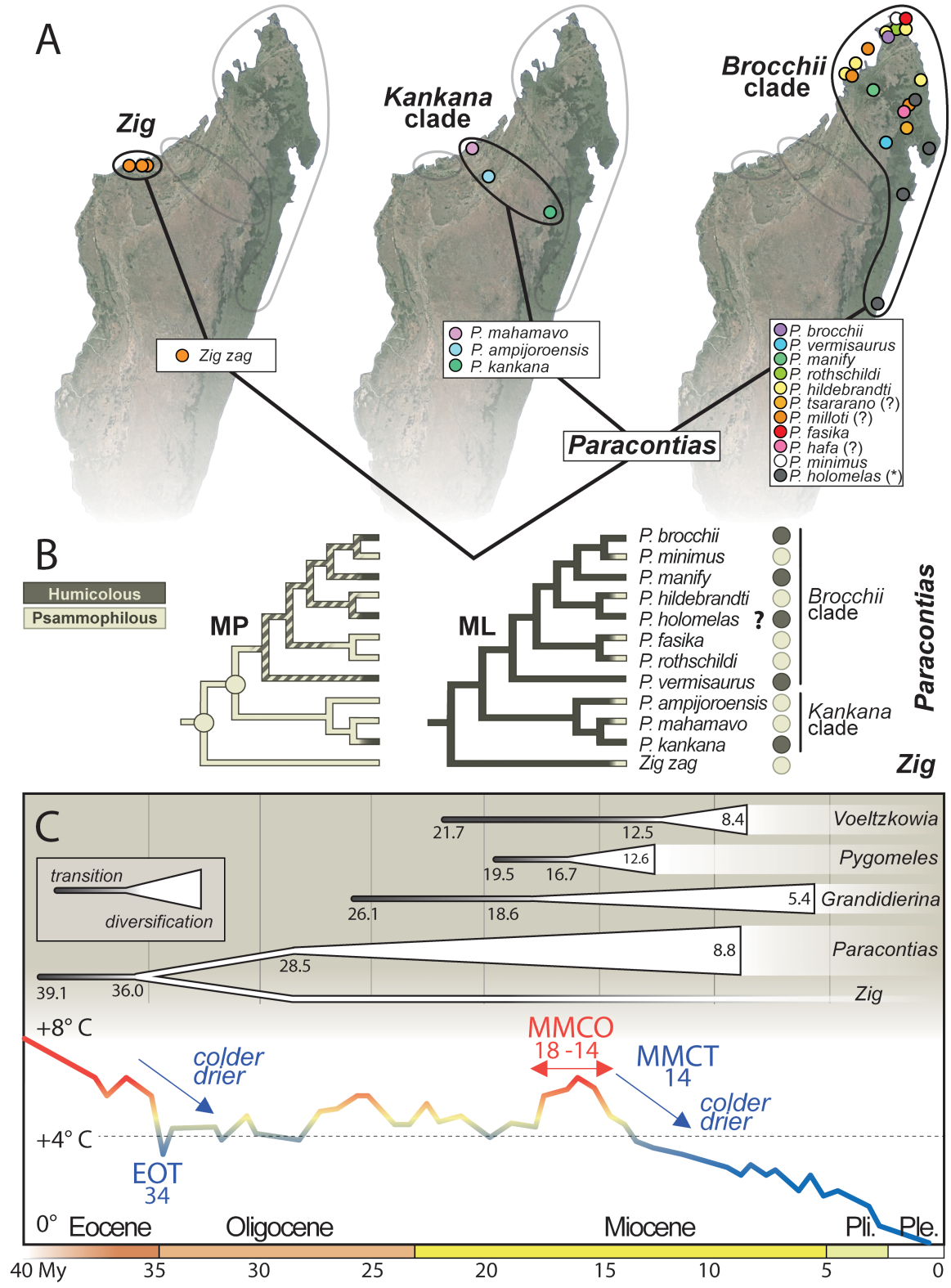

FIGURE 13. Evolution of the "*Zig-Paracontias*" (*ZiPa*) clade. (A) The *ZiPa* clade includes three main lineages with separate ranges: the Brocchii and Kankana clades of *Paracontias* and *Zig* **gen. nov.** The range of *P. holomelas* is not shown due to uncertainties in its identification and distribution (see Miralles *et al.* 2016). Three unsequenced species are tentatively assigned to the *Brocchii* clade based on morphology ("?"). (B) Ancestral state reconstructions based on Maximum parcimony (MP: "ancient origin of psammophyly" hypothesis) and on Maximum Likelyhood (ML: "recent origin" hypothesis). (C) Chronological origin of Madagascar's sand-swimming skinks representing the maximal temporal windows for fossorial specialization (i.e. body elongation and limb reduction, black bars) and the temporal window during which each taxa likely diversified (white triangle). Time in millions of years (My). Expected mean temperature on Earth compared to today (Hansen *et al.* 2013), EOT and MMCT (Eocene-Oligocene and Mid-Miocene climatic transitions), MMCO (Middle Miocene climatic optimum).

recently, at the earliest around the Middle Miocene Climatic Optimum (MMCO, ~18 to 14 Ma) or later, as evidenced by the splits between *Paracontias fasika* and *P. rothschildi* (16.0 Ma), *P. hildebrandti* and *P. holomelas* (14.1 Ma), *P. kankana* and *P. mahamavo* (10.8 Ma) and *P. brocchii* and *P. minimus* (8.8 Ma). Under this hypothesis, the transformational episodes would be temporally congruent with analogous shifts observed in three other Malagasy sand swimming skink lineages: *Grandidierina*, *Voeltzkowia*, and *Pygomeles*, have independently evolved limbless and sand-fossorial morphologies, and are all geographically restricted to the Great White Sand Belt of Madagascar. According to the "recent hypothesis", the near simultaneous emergence of these sand-fossorial lineages points to a common response to shared environmental pressures, most likely the aridification and cooling linked to the Mid-Miocene Climatic Transition (MMCT, ~14 Ma; Miralles *et al.*, 2025).

(2) Ancestral hypothesis. Alternatively, the MP reconstruction unambiguously suggests that the psammophilous state was ancestral for the *ZiPa* clade (i.e., the two most basal nodes; Fig. 13B). Under this scenario, early members of the clade would already have adapted to sandy, fossorial environments. The transition from a fully limbed pentadactyl ancestor to a limbless body form would therefore be directly linked to the adoption of a psammophilic lifestyle (although it remains unclear whether sandy habitat use drove limb reduction, whether limb reduction preceded habitat shift, or whether both processes occured simultaneously). This pattern mirrors that seen the three other Malagasy fossorial skink genera, exclusively psammophilous and inhabiting the Great White Sand Belt of Madagascar (*Grandidierina, Voeltzkowia,* and *Pygomeles*). However, despite the clear parallelism between the *ZiPa* clade and other sand-swimming Malagasy skinks, the MP ancestral state reconstruction suggests that the ancestral adaptation of the *ZiPa* clade to a psammophilous lifestyle occurred substantially earlier (Fig. 13C): The sand-swimmer genera *Grandidierina*, *Voelzkowia* and *Pygomeles* have indeed all likely emerged relatively recently and synchronously during the Mid-Miocene climatic transition (MMCT, ~14 Ma, Miralles *et al.* 2025). Contrastingly, the *ZiPa* clade origin coincides relatively well with the Eocene-Oligocene Transition (EOT, ~34 Ma). Often presented as a dramatic climate shift from a largely ice-free greenhouse world to an icehouse climate (Liu *et al.* 2009; Lauretano *et al.* 2021; Sun *et al.* 2022), the EOT global cooling involved the first major glaciation of Antarctica and a large-scale extinction and floral and faunal turnover (Costa *et al.* 2011; Hernández-Hernández *et al.* 2014; Weppe *et al.* 2021). Studies indicate that the period was marked by a major extinction and subsequent recovery of lemuriform primates (Godfrey *et al.* 2020), as well as the establishment of xeric spiny bush vegetation in western Madagascar resembling the flora found in the subarid southern regions today (Buerki *et al.* 2013; Masters *et al.* 2021). Under this hypothesis, it is tempting to draw parallels between the OET and MMCT. Both periods were indeed characterized by drastic climatic shifts (global cooling, and likely increased aridification in Madagascar) and both would coincide with the emergence of convergent, limbless sand-swimming skinks on the island. This supports a scenario in which an initial phase of cooling and aridification (OET) gave rise to the *ZiPa* clade, followed approximately 20 My later by a second, comparable climatic event (MMCT) that triggered the independent evolution of three additional sand-swimmer lineages (i.e. *Grandidierina*, *Voeltzkowia* and *Pygomeles;* Miralles *et al.* 2025).

To conclude, the stark contrast between these two alternative hypotheses prevents this study from reaching a definitive outcome. On one hand, the "ancient hypothesis" is compelling, as it supports a scenario in which fossoriality in *Zig zag* originated directly as an adaptation to sandy environments, consistent with what has been observed in other Malagasy legless psammophilous skinks. On the other hand, unlike the "recent hypothesis", it fails to explain why all psammophilous species within the *ZiPa* clade (such as *Z. zag*, *P. mahamavo*, *P. ampijoroensis*, *P. minimus*, *P. hildebrandti*, *P. rothschildi*, and *P. fasika*) are found in distinct regions of the white sand belt, despite the fact that, under this scenario, these taxa would have originated well before the formation of this habitat. To address this unresolved issue, the most promising approach would be to expand phylogenetic sampling to eventually enabling a robust reconstruction of ancestral states. This can be achieved by incorporating species that have not yet been included in molecular phylogenetic analyses (e.g., *P. tsararano, P. hafa*) or, as exemplified by this study, by identifying new and highly divergent taxa that are phylogenetically anchored at the base of the clade.

What makes White Sand ecosystems so special for fossorial squamates ?

Except for those present in protected areas (e.g. Ankarafantsika; Ramanamanjato & Rabibisoa 2002), many of the WS areas present in Madagascar have received little attention from field biologists. Most often, they have been sampled only opportunistically and locally, if at all. Yet, WS areas in other tropical environments are known to be fragile and precious for the particular biodiversity they harbor. Different inland WS forest habitats are known around the world (such as Florida sand scrub, Amazonian WS savannah, Indonesian Keranga). Most often, these habitats are characterized by low-nutrient, acidic and very well-drained quartz sandy soils (Kerfahi *et al.* 2019; Sellan *et al.* 2019; Schmalzer & Foster 2020). Compared to other ecosystems in the same regions, they tend to present a lower species diversity, but also a higher level of endemism in the flora and fauna and likely—at least in Madagascar—a higher phylogenetic diversity (Soulebeau *et al.* 2016; Costa *et al.* 2020). Although a synthesis of their invertebrate fauna does not exist, some taxa such as ghost spiders of the genus *Ocyale* appear to be specialized to WS (Jocque *et al.* 2017). As WS substrates do not retain moisture, they are also more vulnerable to wildfires than the adjacent areas and would also present low regeneration capacity (Flores & Holmgren 2021; Percival

et al. 2024). It is well-known that many plants are highly sensitive to the physico-chemical properties of soils, and this no doubt goes a long way towards explaining the establishment of a flora specific to the different kind of sandy soils in Madagascar (e.g. Razanaka 1996; Hanes *et al.* 2022; see also Henschel & Jürgens,in press). In Ankarafantsika, white and red sands are for instance closely associated with specific vegetation types (dry dense forest for the white sands, savannah grasslands for the red sands; Mietton *et al.* 2014). In the same line, the succulent bush *Pachypodium rosulatum* ssp. *rosulatum* and the different herbaceous species forming the genus *Phialiphora* are apparently only known from the inland WS corridor encircling the Mahajanga basin (Lüthy & Lavranos 2005; De Block *et al.* 2020).

Why Malagasy sand fossorial squamates, here represented by distinct lineages distributed in different regions of the island (i.e. *Grandierina*, *Voeltzkowia*, *Pseudoacontias*, some species of *Paracontias* and *Zig*), have apparently so frequently thrived and diversified in WS habitats remains an open question (Fig. 2). It is all the more intriguing as other species of sand-swimming legless lizards, elsewhere in the world, have shown similar preference for WS, such as the skinks *Typhlosaurus lomii* in South Africa, *Pleistodon reynoldsi* in Florida, some species of *Lerista* in Australia, or south American skink-like sand-swimming gymnophtalmid lizards of the genera *Bachia* and *Calyptommatus* (Bauer *et al.* 1999; Smith & Adams 2007; Rodrigues *et al.* 2008; Wieczorek 2021; Uchôa *et al.* 2022). What could make these soils so special, in comparison with other sandy areas of different colors (red, brown or ochre), which are yet very common across Madagascar?

A first explanation is that this pattern may reflect a biased observation: WS surfaces might simply be better preserved than the surrounding areas and therefore more often prospected by field biologists, either because these areas, known to be very low in fertility, are spared from agriculture, or because some of them are located in protected areas. This hypothesis however does not seem very convincing given the very rare occasions when sand-swimmers have been found elsewhere than in WS areas. The high drainage capacity of WS can also be part of the explanation (Fig. 12). During the rainy season, and more particularly during cyclones, heavy rainfall can lead to important flooding in the arid west of Madagascar. Apart from the paroxysmal risk of drowning, waterlogged sand loses its granular fluidity, and is very likely to immobilize small fossorial species, as they are trapped in a muddy sand substrate. A sand that does not retain water and dries quickly after the rain might therefore represent an obvious advantage for these species so closely tied to the physical nature of the substrate in which they move, predate and reproduce. Lastly, a third possible explanation relies on the very high albedo of the white quartzic sands (i.e. the percentage of incident solar radiation reflected) and its consequences in terms of thermal ecology. During our fieldwork in these areas, we indeed experienced particularly arduous conditions due to the intense reflection of the sun's rays on the pristine white surface (oppressive heat, dazzling UV radiation, Fig. 12). Conversely, but for the same reason, white sand ground substrates could be significantly cooler than those of darker colors. In the White Sands National Park (USA), Fishman *et al.* (1994) have indeed shown that the high albedo of the white soil surface (0.60) has a measurable impact on local temperatures, compared with other surrounding darker soil (0.20). On average, in summer and during daytime, the soil temperature (1 cm below surface) was for instance 5 to 15°C cooler in WS area than in the surrounding darker areas. As just a few degrees of temperature can make the difference between optimal and lethal temperature in reptiles (Huey & Bennett 1987), such differences should clearly have profound impact for sand fossorial skinks, whose thermoregulation—like that of fishes in water—depends entirely on the temperature of the substrate in which they are immersed (see also Hays *et al.* 2001).

Conclusions

Our study confirms that the western region of Madagascar, while drier and less species-rich than the east, still supports a herpetological biodiversity that is rich, diverse, and partly undiscovered. Due to their small size and secretive habits, new sand-burrowing taxa likely remain to be discovered within the many isolated and unexplored patches of white sand scattered across western Madagascar. Notably, this research highlights the northwest of the island as a potential center for biotic specialization and diversification within the *ZiPa* clade, thus revealing a previously unrecognized biogeographical pattern (see Brown *et al.* 2016). It also demonstrates that the unconsolidated white sand habitats in this region harbor ancient, highly specialized, and microendemic reptile species.

However, the incomplete geological and paleontological record considerably limits our ability to fully evaluate the impact of Cenozoic climatic fluctuations on this pattern, and several key questions remain unanswered: What was the intensity of these climatic events? How long did they persist? And how widespread were their effects across Madagascar? As illustrated by this study, integrative approaches that combine phylogeography and molecular dating (especially focusing on diverse taxa highly adapted to Madagascar's most arid zones) could provide critical insights to deepen our understanding of these processes.

Competing interests

The authors have declared that no competing interests exist.

Fundings

Funding to A.M. and M.V. was provided by the Deutsche Forschungsgemeinschaft (grant MI 2748/1-1) and to A.

M. by the Agence Nationale de la Recherche (ANR-24-CPJ1-0129-01). Tomographic analyses were possible thanks the project e-COL+ Valorisation des données naturalistes, which received financial support from the French government under the management of the Agence Nationale de la Recherche, as part of the Investments for the Future Program (ANR-21-ESRE-0053) and thanks to the AST-RX, X-ray tomography platform at the MNHN, UAR DoHNEE-CNRS.

Acknowledgments

We are grateful to local teams of Madagascar National Parks, in particular to Jocelyn Bezara, to Andolalao Rakotoarison and Delina Razafimanafo, for their invaluable logistical assistance, and to Nary, our driver from the Madagascar Institute for the Conservation of Tropical Environments (MICET). Many thanks to Laila Rothe, who helped with molecular laboratory work, Marta Bellato, for her help in taking Cscan images, Gregory Schneider, who communicated us pictures of UMMZ specimens and to Mathilde Aladini, Jérome Courtois, Stéphane Grosjean and Nicolas Vidal for their daily help and technical guidance with the MNHN herpetological Collection. We also express our sincere gratitude to Antoine Delauney and André Freiwald for sharing with us their sedimentological expertise (as well as for the photographs and analytical work provided), and to Achille P. Raselimanana, Mark D. Scherz and Angelica Crottini for the stimulating discussions on white sands habitats we have had together over the past years. Aaron Bauer and Mariana Marques provided valuable comments that helped to improve the manuscript. Fieldwork was carried out in the framework of a collaboration accord between the Technische Universität Braunschweig (Zoological Institute), the Université d'Antananarivo, and the Ministry of the Environment, Water and Forests of the Republic of Madagascar. We thank the Malagasy authorities, in particular the "Ministère de l'Environnement et du Développement Durable" and Madagascar National Parks, for research, collection, and export permits.

Authors contributions

A.M. and M.V. conceived the study, A.M., N.A.R., F.B., J.K., F.M.R., M.V. and F.G. collected biological material studied in the present study. A.M., R.S. and E.M. produced raw datasets. A.M., R.S. and F.B. carried out data analyses. A.M. interpreted all data and drafted the original manuscript. All authors contributed to the final manuscript and gave final approval for its submission and publication in its current form.

References

Andreone, F. & Greer, A.E. (2002) Malagasy scincid lizards: descriptions of nine new species, with notes on the morphology, reproduction and taxonomy of some previously described species (Reptilia, Squamata: Scincidae). *Journal of Zoology*, 258, 139–181. https://doi.org/10.1017/S0952836902001280

Angel, F. (1924) Sur une forme nouvelle de lézard, en provenance de Madagascar, appartenant au genre *Grandidierina* (Famille des Scincidés). *Bulletin du Muséum d'histoire naturelle (Paris)*, 30, 450–452.

Angel, F. (1930) Diagnoses d'espèces nouvelles de lézards de Madagascar, appartenant au genre *Scelotes*. *Bulletin du Muséum d'histoire naturelle (Paris)*, (2) 2 (5), 506–509.

Angel, F. (1934) Lézards nouveaux de Madagascar appartenant au genre *Scelotes*. *Bulletin de la Société Zoologique de France*, 41, 294–296.

Angel, F. (1949) Description d'une espèce nouvelle du genre *Paracontias*. *Mémoires de L'Institut Scientifique de Madagascar*, 3 (1), 81–87.

Antonelli, A., Smith, R.J., Perrigo, A.L., Crottini, A., Hackel, J., Testo, W., Farooq, H., Torres Jiménez, M.F., Andela, N., Andermann, T., Andriamanohera, A.M., Andriambololonera, S., Bachman, S.P., Bacon, C.D., Baker, W.J., Belluardo, F., Birkinshaw, C., Borrell, J.S., Cable, S., Canales, N.A., Carrillo, J.D., Clegg, R., Clubbe, C., Cooke, R.S.C., Damasco, G., Dhanda, S., Edler, D., Faurby, S., de Lima Ferreira, P., Fisher, B.L., Forest, F., Gardiner, L.M., Goodman, S.M., Grace, O.M., Guedes, T.B., Henniges, M.C., Hill, R., Lehmann, C.E.R., Lowry, P.P., Marline, L., Matos-Maraví, P., Moat, J., Neves, B., Nogueira, M.G.C., Onstein, R.E., Papadopulos, A.S.T., Perez-Escobar, O.A., Phelps, L.N., Phillipson, P.B., Pironon, S., Przelomska, N.A.S., Rabarimanarivo, M., Rabehevitra, D., Raharimampionona, J., Rajaonah, M.T., Rajaonary, F., Rajaovelona, L.R., Rakotoarinivo, M., Rakotoarisoa, A.A., Rakotoarisoa, S.E., Rakotomalala, H.N., Rakotonasolo, F., Ralaiveloarisoa, B.A., Ramirez-Herranz, M., Randriamamonjy, J.E.N., Randriamboavonjy, T., Randrianasolo, V., Rasolohery, A., Ratsifandrihamanana, A.N., Ravololomanana, N., Razafiniary, V., Razanajatovo, H., Razanatsoa, E., Rivers, M., Sayol, F., Silvestro, D., Vorontsova, M.S., Walker, K., Walker, B.E., Wilkin, P., Williams, J. & Ziegler, T., Zizka, A. & Ralimanana, H. (2022) Madagascar's extraordinary biodiversity: Evolution, distribution, and use. *Science*, 378 (6623), eabf0869. https://doi.org/10.1126/science.abf0869

Bauer, A.M., Schneider, V., Lamb, T., Moler, P.E. & Babb, R.D. (1999) New data on the South African acontine skink *Typhlosaurus lomii* Haacke 1986 (Squamata: Scincidae). *African Journal of Herpetology*, 48 (1–2), 21–25. https://doi.org/10.1080/21564574.1999.9651067

Beaulieu, J.M. & O'Meara, B.C. (2016) Detecting hidden diversification shifts in models of trait-dependent speciation and extinction. *Systematic Biology*, 65, 583–601. https://doi.org/10.1093/sysbio/syw022

Belluardo, F., Muñoz-Pajares, A.J., Miralles, A., Silvestro, D., Cocca, W., Ratsoavina, F.M., Villa, A., Roberts, S.H., Mezzasalma, M., Zizka, A., Antonelli, A. & Crottini, A. (2023) Slow and steady wins the race: Diversification rate is independent from body size and lifestyle in Malagasy skinks (Squamata: Scincidae: Scincinae). *Molecular Phylogenetics and Evolution*, 178, 107635. https://doi.org/10.1016/j.ympev.2022.107635

Bocage, J.V.B. du (1889) Mélanges erpétologiques. I. Sur un Scincoidien nouveau de Madagascar. *Jornal de sciências mathemáticas, físicas e naturais (Lisboa)*, 2 (2), 125–126.

Boettger, O. (1881) Diagnoses reptilium et batrachiorum novorum ab ill. Antonio Stumpff in insula Nossi-Bé Madagascariensi lectorum. *Zoologischer Anzeiger*, 4 (87), 358–362.

Boettger, O. (1882) Diagnoses Reptilium et Batrachiorum Novorum insulae Nossi Be Madagascariensis. *Zoologischer Anzeiger*, 5, 478–480.

Boettger, O. (1893) *Katalog der Reptilien-Sammlung im Museum der Senckenbergischen Naturforschenden Gesellschaft in Frankfurt am Main. I. Teil (Rhynchocephalen, Schildkröten, Krokodile, Eidechsen, Chamäleons)*. Gebrüder Knauer, Frankfurt a. M., 140 pp.

Bouckaert, R., Vaughan, T.G., Barido-Sottani, J., Duchêne, S., Fourment, M., Gavryushkina, A., Heled, J., Jones, G., Kühnert, D., De Maio, N., Matschiner, M., Mendes, F.K., Müller, N.F., Ogilvie, H.A., Du Plessis, L., Popinga, A., Rambaut, A., Rasmussen, D., Siveroni, I., Suchard, M.A., Wu, C.H., Xie, D. & Zhang, C. (2019) BEAST 2.5: An advanced software platform for Bayesian evolutionary analysis. *PLoS Computational Biology*, 15, e1006650. https://doi.org/10.1371/journal.pcbi.1006650

Boulenger, G.A. (1887) *Catalogue of the lizards in the British Museum (Nat. Hist.) III. Lacertidae, Gerrhosauridae, Scincidae, Anelytropsidae, Dibamidae, Chamaeleontidae*. London, 575 pp.

Boulenger, G.A. (1888) XIII – Descriptions of new Reptiles and Batrachians from Madagascar. *The Annals and Magazine of Natural History*, 1 (2), 101–107. https://doi.org/10.1080/00222938809460688

Boulenger, G.A. (1889) XXIX – Descriptions of new reptiles and batrachians from Madagascar. *The Annals and Magazine of Natural History*, 4 (21), 244–248. https://doi.org/10.1080/00222938909460511

Boulenger, G.A. (1896) LXII – Descriptions of new lizards from Madagascar. *The Annals and Magazine of Natural History*, 17 (102), 444–449. https://doi.org/10.1080/00222939608680395

Boumans, L., Vieites, D.R., Glaw, F. & Vences, M. (2007) Geographical patterns of deep mitochondrial differentiation in widespread Malagasy reptiles. *Molecular Phylogenetics and Evolution*, 45, 822–839. https://doi.org/10.1016/j.ympev.2007.05.028

Brelsford, A., Dufresnes, C. & Perrin, N. (2016) High-density sex-specific linkage maps of a European tree frog (*Hyla arborea*) identify the sex chromosome without information on offspring sex. *Heredity*, 116 (2), 177–181. https://doi.org/10.1038/hdy.2015.83

Brown, J.L., Sillero, N., Glaw, F., Bora, P., Vieites, D.R. & Vences, M. (2016) Spatial biodiversity patterns of Madagascar's amphibians and reptiles. *PLoS One*, 11, e0144076. https://doi.org/10.1371/journal.pone.0144076

Brygoo, E.R. (1980) Systématique des lézards scincidés de la région malgache. III. Les « Acontias » de Madagascar: *Pseudoacontias* Barboza du Bocage, 1889, *Paracontias* Mocquard, 1894, *Pseudoacontias* Hewitt, 1929, et *Malacontias* Greer, 1970. IV. *Amphiglossus reticulatus* (Kaudern, 1922) nov. comb., troisième espèce du genre; ses rapports avec *Amphiglossus waterloti* (Angel, 1920). *Bulletin du Muséum national d'Histoire Naturelle, Section A*, 2 (3), 905–918.

Brygoo, E.R. (1981) Systématique des lézards scincidés de la région malgache. VI. Deux scincinés nouveaux. *Bulletin du Muséum national d'Histoire naturelle, section A*, 3 (1), 261–268. https://doi.org/10.5962/p.285822

Buerki, S., Devey, D.S., Callmander, M.V., Phillipson, P.B. & Forest, F. (2013) Spatio-temporal history of the endemic genera of Madagascar. *Botanical Journal of the Linnean Society*, 171 (2), 304–329. https://doi.org/10.1111/boj.12008

Burnham, K.P. & Anderson, D.R. (2002) *Model Selection and Multimodel Inference: A Practical Information-Theoretic Approach*, second ed. Springer, New York, 515 pp.

Catchen, J., Hohenlohe, P.A., Bassham, S., Amores, A. & Cresko, W.A. (2013) Stacks: an analysis tool set for population genomics. *Molecular Ecology*, 22, 3124–3140. https://doi.org/10.1111/mec.12354

Conroy, C.J., Papenfuss, T., Parker, J. & Hahn, N. (2009) Use of tricaine methanesulfonate (MS-222) for euthanasia of reptiles. *Journal of the American Association for Laboratory Animal Science*, 48, 28–32.

Costa, E., Garcés, M., Sáez, A., Cabrera, L. & López-Blanco, M. (2011) The age of the "Grande Coupure" mammal turnover: New constraints from the Eocene–Oligocene record of the Eastern Ebro Basin (NE Spain). *Palaeogeography, Palaeoclimatology, Palaeoecology*, 301, 97–107. https://doi.org/10.1016/j.palaeo.2011.01.005

Costa, F.M., Terra-Araujo, M.H., Zartman, C.E., Cornelius, C., Carvalho, F.A., Hopkins, M.J.G., Viana, P.L., Prata, E.M.B. & Vicentini, A. (2020) Islands in a green ocean: Spatially structured endemism in Amazonian white-sand vegetation. *Biotropica*, 52 (1), 34–45. https://doi.org/10.1111/btp.12732

Crottini, A., Dordel, J., Köhler, J., Glaw, F., Schmitz, A. & Vences, M. (2009) A multilocus phylogeny of Malagasy scincid lizards elucidates the relationships of the fossorial genera *Androngo* and *Cryptoscincus*. *Molecular Phylogenetics and Evolution*, 53, 345–350. https://doi.org/10.1016/j.ympev.2009.05.024

De Block, P., Rakotonasolo, F., Vrijdaghs, A. & Dessein, S. (2020) Two new species of *Phialiphora* (Spermacoceae, Rubiaceae) exemplify drought adaptations in western Madagascar. *Plant Ecology and Evolution*, 153 (2), 267–282. https://doi.org/10.5091/plecevo.2020.1675

Duméril, A.M.C. & Bibron, G. (1839) *Erpétologie Générale ou Histoire Naturelle Complète des Reptiles. Vol. 5*. Roret, Fain et Thunot, Paris, 871 pp.

Erens, J., Miralles, A., Glaw, F., Chatrou, L. & Vences, M. (2017) Extended molecular phylogenetics and revised systematics of Malagasy scincine lizards. *Molecular Phylogenetics and Evolution*, 107, 466–472. https://doi.org/10.1016/j.ympev.2016.12.008

Fishman, B., Taha, H. & Akbari, H. (1994) Meso-Scale Cooling Effects of High Albedo Surfaces: Analysis of Meteorological Data from White Sands National Monument and White Sands Missile Range. *Lawrence Berkeley National Laboratory*. LBNL Report #: LBL-35056. Available from: https://escholarship.org/uc/item/1kh4b67k (accessed 01 October 2025) https://doi.org/10.2172/10180636

Flores, B.M. & Holmgren, M. (2021) White-Sand savannas expand at the core of the Amazon after forest wildfires. *Ecosystems*, 24 (7), 1624–1637.
https://doi.org/10.1007/s10021-021-00607-x

Glaw, F. & Vences, M. (2007) A Field Guide to the Amphibians and Reptiles of Madagascar. Third edition. Vences and Glaw Verlag, Cologne, 496 pp.

Godfrey, L.R., Samonds, K.E., Baldwin, J.W., Sutherland, M.R., Kamilar, J.M. & Allfisher, K.L. (2020) Mid-Cenozoic climate change, extinction, and faunal turnover in Madagascar, and their bearing on the evolution of lemurs. *BMC Evolutionary Biology*, 20 (97).
https://doi.org/10.1186/s12862-020-01628-1

Grandidier, A. (1867) Liste des reptiles nouveaux découverts, en 1866, sur la côte sud-ouest de Madagascar. *Revue et Magazine de Zoologie (Paris)*, Série 2, 19, 232–234.

Grandidier, A. (1869) Descriptions de quelques animaux nouveaux découverts, pendant l'année 1869, sur la côte ouest de Madagascar. *Revue et Magazine de Zooogie (Paris)*, Série 2, 21, 337–342.

Grandidier, A. (1872) Descriptions de quelques Reptiles nouveaux découverts à Madagascar en 1870. *Annales des Sciences Naturelles, Zoologie et Paléontologie*, 15 (5), 6–11.

Guindon, S., Dufayard, J.-F., Lefort, V., Anisimova, M., Hordijk, W. & Gascuel, O. (2010) New algorithms and methods to estimate maximum-likelihood phylogenies: Assessing the performance of PhyML 3.0. *Systematic Biology*, 59 (3), 307–321.
https://doi.org/10.1093/sysbio/syq010

Günther, A. (1877) Descriptions of some new species of reptiles from Madagascar. *The Annals and Magazine of Natural History*, 19 (112), 313–317.
https://doi.org/10.1080/00222937708682150

Hanes, M.M., Shell, S., Shimu, T., Crist, C. & Machkour-M'Rabet, S. (2022) The phylogeographic history of *Megistostegium* (Malvaceae) in the dry, spiny thickets of southwestern Madagascar using RAD-seq data and ecological niche modeling. *Ecology and Evolution*, 12, e8632.
https://doi.org/10.1002/ece3.8632

Hansen, J., Sato, M., Russell, G. & Kharecha, P. (2013) Climate sensitivity, sea level and atmospheric carbon dioxide. *Philosophical Transactions of the Royal Society A: Mathematical, Physical and Engineering Sciences*, 371 (2001), 20120294.
https://doi.org/10.1098/rsta.2012.0294

Hays, G.C., Ashworth, J.S., Barnsley, M.J., Broderick, A.C., Emery, D.R., Godley, B.J., Henwood, A. & Jones, E.L. (2001) The importance of sand albedo for the thermal conditions on sea turtle nesting beaches. *Oikos*, 93, 87–94.
https://doi.org/10.1034/j.1600-0706.2001.930109.x

Henschel, J.R. & Jürgens, N. (in press) Ecology of psammophily in the Namib dunes. *In*: Eckhardt, F.D., Livingstone, I. & Thomas, D.S.G. (Eds.), *Southern African Dunes*. Springer.

Hernández-Hernández, T., Brown, J.W., Schlumpberger, B.O., Eguiarte, L.E. & Magallón, S. (2014) Beyond aridification: multiple explanations for the elevated diversification of cacti in the New World Succulent Biome. *New Phytologist*, 202, 1382–1397.
https://doi.org/10.1111/nph.12752

Hoang, D.T., Chernomor, O., Von Haeseler, A., Minh, B.Q. & Vinh, L.S. (2018) UFBoot2: improving the ultrafast bootstrap approximation. *Molecular Biology and Evolution*, 35 (2), 518–522.
https://doi.org/10.1093/molbev/msx281

Huey, R.B., Pianka, E.R., Egan, M.E. & Coons, L.W. (1974) Ecological shifts in sympatry: Kalahari fossorial lizards (*Typhlosaurus*). *Ecology*, 55, 304–316.
https://doi.org/10.2307/1935218

Huey, R.B. & Bennett, A.F. (1987) Phylogenetic studies of coadaptation: preferred temperatures versus optimal performance temperatures of lizards. *Evolution*, 41 (5), 1098–1115.
https://doi.org/10.1111/j.1558-5646.1987.tb05879.x

IUCN Standards and Petitions Committee (2024) Guidelines for Using the IUCN Red List Categories and Criteria. Version 16. Prepared by the Standards and Petitions Committee. Available from: https://www.iucnredlist.org/resources/redlistguidelines (accessed 1 October 2025)

Jocque, M., Wellens, S., Andrianarivosoa, J.D., Rakotondraparany, F., The Seing, S. & Jocqué, R. (2017) A new species of *Ocyale* (Araneae, Lycosidae) from Madagascar, with first observations on the biology of a representative in the genus. *European Journal of Taxonomy*, 355, 1–13.
https://doi.org/10.5852/ejt.2017.355

Kaffenberger, N., Wollenberg, K.C., Köhler, J., Glaw, F., Vieites, D.R. & Vences, M. (2012) Molecular phylogeny and biogeography of Malagasy frogs of the genus *Gephyromantis*. *Molecular Phylogenetics and Evolution*, 62, 555–560.
https://doi.org/10.1016/j.ympev.2011.09.023

Kalyaanamoorthy, S., Minh, B.Q., Wong, T.K., Von Haeseler, A. & Jermiin, L.S. (2017) ModelFinder: fast model selection for accurate phylogenetic estimates. *Nature Methods*, 14 (6), 587–589.
https://doi.org/10.1038/nmeth.4285

Katoh, K. & Standley, D.M. (2013) MAFFT Multiple Sequence Alignment Software version 7: Improvements in performance and usability. *Molecular Biology and Evolution*, 30, 772–780.
https://doi.org/10.1093/molbev/mst010

Kaudern, W. (1922) Sauropsiden aus Madagascar. *Zoologische Jahrbücher. Abteilung für Systematik, Geographie und Biologie der Tiere*, 45, 395–458.
https://doi.org/10.5962/bhl.part.5180

Kerfahi, D., Tripathi, B.M., Slik, J.W.F., Sukri, R.S., Jaafar, S., Dong, K., Ogwu, M.C., Kim, H.-K. & Adams, J.M. (2019) Soil metagenome of tropical white sand heath forests in Borneo: what functional traits are associated with an extreme environment within the tropical rainforest? *Pedosphere*, 29 (1), 12–23.
https://doi.org/10.1016/S1002-0160(18)60054-2

Köhler, J., Vences, M., Erbacher, M. & Glaw, F. (2010) Systematics of limbless scincid lizards from northern Madagascar: morphology, phylogenetic relationships and implications for classification (Squamata: Scincidae). *Organisms Diversity and Evolution*, 10, 147–159.
https://doi.org/10.1007/s13127-010-0011-5

Köhler, J., Vieites, D.R., Glaw, F., Kaffenberger, N. & Vences, M. (2009) A further new species of limbless skink, genus *Paracontias*, from eastern Madagascar. *African Journal of Herpetology*, 58, 98–105.

https://doi.org/10.1080/21564574.2009.9650029

Lanfear, R., Frandsen, P.B., Wright, A.M., Senfeld, T. & Calcott, B. (2016) PartitionFinder 2: new methods for selecting partitioned models of evolution formolecular and morphological phylogenetic analyses. *Molecular Biology and Evolution*, 34, 772–773.
https://doi.org/10.1093/molbev/msw260

Lauretano, V., Kennedy-Asser, A.T., Korasidis, V.A., Wallace, M.W., Valdes, P.J., Lunt, D.J., Pancost, R.D. & Naafs, B.D.A. (2021) Eocene to Oligocene terrestrial Southern Hemisphere cooling caused by declining *p*CO2. *Nature Geoscience*, 14, 659–664.
https://doi.org/10.1038/s41561-021-00788-z

Liu, Z., Pagani, M., Zinniker, D., Deconto, R., Huber, M., Brinkhuis, H., Shah, S.R., Leckie, R.M. & Pearson, A. (2009) Global Cooling During the Eocene-Oligocene Climate Transition. *Science*, 323, 1187–1190.
https://doi.org/10.1126/science.1166368

Lüthy, J. & Lavranos, J. (2005) *Pachypodium rosulatum* ssp *bemarahense* a new subspecies from Madagascar. *Cactus and Succulent Journal*, 77 (1), 38–42.
https://doi.org/10.2985/0007-9367(2005)77[38:PRSBAN]2.0.CO;2

Maddison, W.P., Midford, P.E. & Otto, S.P. (2007) Estimating a binary character's effect on speciation and extinction. *Systematic Biology*, 56, 701–710.
https://doi.org/10.1080/10635150701607033

Maddison, W.P. & Maddison, D.R. (2023) Mesquite: a modular system for evolutionary analysis. Version 3.81. Available from: http://www.mesquiteproject.org (accessed 1 October 2025)

Mahony, S., Kamei, R.G., Brown, R.M. & Chan, K.O. (2024) Unnecessary splitting of genus-level clades reduces taxonomic stability in amphibians. *Vertebrate Zoology*, 74, 249–277.
https://doi.org/10.3897/vz.74.e114285

Masters, J.C., Génin, F., Zhang, Y., Pellen, R., Huck, T., Mazza, P.P.A., Rabineau, M., Doucouré, M. & Aslanian, D. (2021) Biogeographic mechanisms involved in the colonization of Madagascar by African vertebrates: Rifting, rafting and runways. *Journal of Biogeography*, 48, 492–510.
https://doi.org/10.1111/jbi.14032

Matschiner, M. (2016) Fitchi: haplotype genealogy graphs based on the Fitch algorithm. *Bioinformatics*, 32 (8), 1250–1252.
https://doi.org/10.1093/bioinformatics/btv717

Mietton, M., Cordier, S., Frechen, M., Dubar, M., Beiner, M. & Andrianaivoarivony, R. (2014) New insights into the age and formation of the Ankarokaroka lavaka and its associated sandy cover (NW Madagascar, Ankarafantsika natural reserve). *Earth Surface Processes and Landforms*, 39, 1467–1477.
https://doi.org/10.1002/esp.3536

Minh, B.Q., Schmidt, H.A., Chernomor, O., Schrempf, D., Woodhams, M.D., Von Haeseler, A. & Lanfear, R. (2020) IQ-TREE 2: new models and efficient methods for phylogenetic inference in the genomic era. *Molecular Biology and Evolution*, 37 (5), 1530–1534.
https://doi.org/10.1093/molbev/msaa015

Miralles, A., Anjeriniana, M., Hipsley, C.A., Müller, J., Glaw, F. & Vences, M. (2012) Variations on a bodyplan: description of a new Malagasy "mermaid skink" with flipper-like forelimbs only (Scincidae: *Sirenoscincus* Sakata & Hikida, 2003). *Zoosystema*, 34 (4), 701–710.
https://doi.org/10.5252/z2012n4a3

Miralles, A., Hipsley, C.A., Erens, J., Gehara, M., Rakotoarison, A., Glaw, F., Müller, J. & Vences, M. (2015) Distinct patterns of desynchronized limb regression in Malagasy scincine lizards (Squamata, Scincidae). *PLoS One*, 10 (6), e0126074.
https://doi.org/10.1371/journal.pone.0126074

Miralles, A., Jono, T., Mori, A., Gandola, R., Erens, J., Köhler, J., Glaw, F. & Vences, M. (2016a) A new perspective on the reduction of cephalic scales in fossorial legless skinks (Squamata, Scincidae). *Zoologica Scripta*, 45 (4), 380–393.
https://doi.org/10.1111/zsc.12164

Miralles, A., Köhler, J., Glaw, F. & Vences, M. (2011c) A molecular phylogeny of the *Madascincus polleni* species complex, with description of a new species of scincid lizard from the coastal dune area of northern Madagascar. *Zootaxa*, 2876, 1–16.
https://doi.org/10.11646/zootaxa.2876.1.1

Miralles, A., Köhler, J., Glaw, F. & Vences, M. (2016b) Species delimitation methods put into taxonomic practice: Two new *Madascincus* species formerly allocated to historical species names (Squamata: Scincidae). *Zoosystematics and Evolution*, 92 (2), 257–275.
https://doi.org/10.3897/zse.92.9945

Miralles, A., Köhler, J., Vieites, D.R., Glaw, F. & Vences, M. (2011b) Hypotheses on rostral shield evolution in fossorial lizards derived from the phylogenetic position of a new species of the *Paracontias* (Scincidae). *Organisms Diversity and Evolution*, 11, 135–150.
https://doi.org/10.1007/s13127-011-0042-6

Miralles, A., Raselimanana, A.P., Rakotomalala, D., Vences, M. & Vieites, D.R. (2011a) A new large and colorful skink of the genus *Amphiglossus* from Madagascar revealed by morphology and multilocus molecular study. *Zootaxa*, 2918, 47–67.
https://doi.org/10.11646/zootaxa.2918.1.5

Miralles, A., Schmidt, R., Rakotoarison, A., Delaunay, A., Freiwald, A., Rahagalala, N.A., Rakotomanga, S., Razafimanafo, D., Ratsoavina, F.M., Crottini, A., Raselimanana, A.P., Glaw, F. & Vences, M. (2025) Integrative taxonomy of Madagascar's sand-swimming skinks (Scincidae: *Voeltzkowia*, *Grandidierina*) and preliminary evidence for an overlooked inland belt of white sand patches across the island's west. *Zoological Journal of the Linnean Society*, 205 (3), zlaf147.
https://doi.org/10.1093/zoolinnean/zlaf147

Miralles, A. & Vences, M. (2013) New metrics for comparison of taxonomies reveal striking discrepancies among species delimitation methods in *Madascincus* lizards. *PLoS One*, 8 (7), e68242.
https://doi.org/10.1371/journal.pone.0068242

Mocquard, F. (1894) Reptiles nouveaux ou insuffisamment connus de Madagascar. *Compte-Rendu sommaire des séances de la Société Philomatique de Paris*, 8 (5–6), 3–10.

Mocquard, F. (1897) Notes herpétologiques. *Bulletin du Muséum d'histoire naturelle (Paris)*, Série 1, 3 (6), 211–217.
https://doi.org/10.5962/p.144947

Mocquard, F. (1901) Note préliminaire sur une collection de reptiles et de batraciens recueillis par M. Alluaud dans le sud de Madagascar. *Bulletin du Muséum d'histoire naturelle (Paris)*, 7, 251–256.
https://doi.org/10.5962/bhl.part.1622

Mocquard, F. (1905) Note préliminaire sur une collection de reptiles et de Batraciens offerte au Muséum par M. Maurice de Rothschild. *Bulletin du Muséum d'histoire naturelle (Paris)*, 11, 285–288.

Mocquard, F. (1906a) Description de quelques reptiles et d'un batracien d'espèces nouvelles. *Bulletin du Muséum d'histoire naturelle (Paris)*, 12 (5), 247–253.

Mocquard, F. (1906b) Description de quelques espèces nouvelles de Reptiles. *Bulletin du Muséum d'histoire naturelle (Paris)*, 12 (7), 464–466.

Mocquard, F. (1908) Description de quelques reptiles et d'un batracien nouveaux de la collection du Muséum. *Bulletin du Muséum d'histoire naturelle (Paris)*, 14, 259–262. https://doi.org/10.5962/bhl.part.5657

Muñoz-Pajares, A.J., Belluardo, F., Cocca, W. & Crottini, A. (2019) PipeLogeny: An automated pipeline for phylogenetic reconstruction. Available from: https://sites.google.com/site/pipelogenydownload/ (accessed 1 November 2024)

Nagy, Z.T., Sonet, G., Glaw, F. & Vences, M. (2012) First large-scale DNA barcoding assessment of reptiles in the biodiversity hotspot of Madagascar, based on newly designed COI primers. *PLoS One*, 7, e34506. https://doi.org/10.1371/journal.pone.0034506

Nussbaum, R.A. & Raxworthy, C.J. (1994) A new species of *Mabuya* Fitzinger (Reptilia: Squamata: Scincidae) from southern Madagascar. *Herpetologica*, 50 (3), 309–319.

Nussbaum, R.A. & Raxworthy, C.J. (1995a) Review of the scincine genus *Pseudoacontias* Barboza du Bocage (Reptilia: Squamata: Scincidae) of Madagascar. *Herpetologica*, 51 (1), 91–99.

Nussbaum, R.A. & Raxworthy, C.J. (1995b) A new *Mabuya* (Reptilia: Squamata: Scincidae) of the *aureopunctata*-group from southern Madagascar. *Journal of Herpetology*, 29 (1), 28–38. https://doi.org/10.2307/1565082

Nussbaum, R.A. & Raxworthy, C.J. (1998a) New long-tailed *Mabuya* Fitzinger from Lokobe Reserve, Nosy Be, Madagascar (Reptilia: Squamata: Scincidae). *Copeia*, 1998 (1), 114–119. https://doi.org/10.2307/1447706

Nussbaum, R.A. & Raxworthy, C.J. (1998b) A new species of *Mabuya* Fitzinger (Reptilia: Squamata: Scincidae) from the High Plateau (Isalo National Park) of South-Central Madagascar. *Herpetologica*, 54 (3), 336–343. https://doi.org/10.2307/1447706

Nussbaum, R.A., Raxworthy, C.J. & Ramanamanjato, J.B. (1999) Additional species of *Mabuya* Fitzinger (Reptilia: Squamata: Scincidae) from Western Madagascar. *Journal of Herpetology*, 33 (2), 264–280. https://doi.org/10.2307/1565724

O'Shaughnessy, A.W.E. (1879) Description of new species of lizards in the collection of the British Museum. *Annals of Natural History and Magazine of Natural History*, (5)4, 295–303. https://doi.org/10.1080/00222937908679832

Paris, J.R., Stevens, J.R. & Catchen, J.M. (2017) Lost in parameter space: A road map for stacks. *Methods in Ecology and Evolution*, 8 (10), 1360–1373. https://doi.org/10.1111/2041-210X.12775

Pasteur, G. & Paulian, R. (1962) Diagnose d'un lézard apode de Madagascar: *Pygomeles petteri* n. sp. (Scincidae). *Bulletin du Muséum national d'Histoire naturelle (Paris)*, Série 2, 34 (1), 66.

Percival, J.E.H., Sato, H., Razanaparany, T.P., Rakotomamonjy, A.H., Razafiarison, Z.L. & Kitajima, K. (2024) Non fire-adapted dry forest of Northwestern Madagascar: Escalating and devastating trends revealed by Landsat timeseries and GEDI lidar data. *PLoS One*, 19 (2), e0290203. https://doi.org/10.1371/journal.pone.0290203

Peters, W.C.H. (1854) Diagnosen neuer Batrachier, welche zusammen mit der früher (24. Juli und 17. August) gegebenen Übersicht der Schlangen und Eidechsen mitgetheilt werden. *Bericht über die zur Bekanntmachung geeigneten Verhandlungen der Königlich Preussische Akademie der Wissenschaften zu Berlin*, 1854, 614–628.

Peters, W. (1880) Über die von Hrn. J. M. Hildebrandt auf Nossi-Bé und Madagascar gasammelten Säugethiere und Amphibien. *Monatsberichte der Königlich Preussischen Akademie der Wissenschaften zu Berlin*, 1880, 508–511.

Ramanamanjato, J.B., Nussbaum, R.A. & Raxworthy, C.J. (1999a) A new species of *Mabuya* Fitzinger (Squamata: Scincidae: Lygosominae) from northern Madagascar. *Occasional Papers of the Museum of Zoology University of Michigan*, 728, 1–22.

Ramanamanjato, J.B., Nussbaum, R.A. & Raxworthy, C.J. (1999b) A new species of *Mabuya* Fitzinger (Reptilia: Squamata: Scincidae) from the Onilahy River of south-west Madagascar. *The Herpetological Journal*, 9 (2), 65–72.

Ramanamanjato, J.B. & Rabibisoa, N. (2002) Evaluation rapide de la diversité biologique des reptiles et amphibiens de la Réserve Naturelle Intégrale d'Ankarafantsika. *In*: Alonso, L.E., Schulenberg, T.S., Radilofe, S. & Missa, O. (Eds.), *Une evaluation biologique de la Réserve Naturelle Intégrale d'Ankarafantsika, Madagascar*. Bulletin RAP d'evaluation rapide 23, Washington : Conservation International, pp. 98–103.

Rambaut, A. (2010) FigTree v1.3.1. Institute of Evolutionary Biology, University of Edinburgh, Edinburgh. Available from: http://tree.bio.ed.ac.uk/software/figtree/ (accessed 20 Nov 2024)

Rambaut, A., Drummond, A.J., Xie, D., Baele, G. & Suchard, M.A. (2018) Posterior summarization in Bayesian phylogenetics using Tracer 1.7. *Systematic Biology*, 67, 901–904. https://doi.org/10.1093/sysbio/syy032

Raxworthy, C.J. & Nussbaum, R.A. (1993) Four new species of *Amphiglossus* from Madagascar (Squamata: Scincidae). *Herpetologica*, 49 (3), 326–341.

Razanaka, S.L. (1996) Répartition des espèces xerophiles dans le sud-ouest de Madagascar. *In*: Lourenço, W.R. (Ed.), *Biogeography of Madagascar. Actes du Colloque International Biogéographie de Madagascar, Société de Biogéographie – Muséum - ORSTOM, Paris: ORSTOM éditions*, pp. 171–176.

R Core Team (2024) R: A Language and Environment for Statistical Computing. R Foundation for Statistical Computing, Vienna, Austria. Available from: https://www.R-project.org/ (accessed 1 October 2025)

Rochette, N.C., Rivera-Colón, A.G. & Catchen, J.M. (2019) Stacks 2: Analytical methods for paired-end sequencing improve RADseq-based population genomics. *Molecular Ecology*, 28 (21), 4737–4754. https://doi.org/10.1111/mec.15253

Rodrigues, M.T., Camacho, A., Nunes, P.M.S., Recoder, R.S., Teixeira, M. Jr., Valdujo, P.H., Ghellere, J.M.B., Mott, T. & Nogueira, C. (2008) A new species of the lizard genus *Bachia* (Squamata: Gymnophthalmidae) from the Cerrados of Central Brazil. *Zootaxa*, 1875 (1), 39–50. https://doi.org/10.11646/zootaxa.1875.1.3

Ronquist, F., Teslenko, M., Van Der Mark, P., Ayres, D.L., Darling, A., Höhna, S., Larget, B., Liu, L., Suchard, M.A. & Huelsenbeck, J.P. (2012) MrBayes 3.2: Efficient Bayesian phylogenetic inference and model choice across a large model space. *Systematic Biology*, 61, 539–542. https://doi.org/10.1093/sysbio/sys029

Sakata, S. & Hikida, T. (2003a) A new fossorial scincine lizard of the genus *Pseudoacontias* (Reptilia: Squamata: Scincidae) from Nosy Be, Madagascar. *Amphibia-Reptilia*, 24 (1), 57–64. https://doi.org/10.1163/156853803763806948

Sakata, S. & Hikida, T. (2003b) A fossorial lizard with forelimbs only: description of a new genus and species of Malagasy skink (Reptilia: Squamata: Scincidae). *Current Herpetology*, 22, 9–15. https://doi.org/10.5358/hsj.22.9

Salzburger, W., Ewing, G.B. & Von Haeseler, A. (2011) The performance of phylogenetic algorithms in estimating haplotype genealogies with migration. *Molecular Ecology*, 20, 1952–1963. https://doi.org/10.1111/j.1365-294X.2011.05066.x

Scherz, M.D., Vences, M., Rakotoarison, A., Andreone, F., Köhler, J., Glaw, F. & Crottini, A. (2017) Lumping or splitting in the Cophylinae (Anura: Microhylidae) and the need for a parsimony of taxonomic changes: a response to Peloso *et al.* (2017). *Salamandra*, 53, 479–483.

Schmalzer, P.A. & Foster, T.E. (2020) Variation of Florida scrub vegetation along gradients of soil pH and landscape age on a barrier island complex. *The Journal of the Torrey Botanical Society*, 147 (2), 140–155. https://doi.org/10.3159/TORREY-D-19-00033.1

Schmitz, A., Brandley, M.C., Mausfeld, P., Vences, M., Glaw, F., Nussbaum, R.A. & Reeder, T.W. (2005) Opening the black box: phylogenetics and morphological evolution of the Malagasy fossorial lizards of the subfamily "Scincinae". *Molecular Phylogenetics and Evolution*, 34 (1), 118–133. https://doi.org/10.1016/j.ympev.2004.08.016

Sellan, G., Thompson, J., Majalap, N. & Brearley, F.Q. (2019) Soil characteristics influence species composition and forest structure differentially among tree size classes in a Bornean heath forest. *Plant Soil*, 438, 173–185. https://doi.org/10.1007/s11104-019-04000-5

Smith, L.A. & Adams, M. (2007) Revision of the *Lerista muelleri* species-group (Lacertilia: Scincidae) in Western Australia, with a redescription of *L. muelleri* (Fischer, 1881) and the description of nine new species. *Records of the Western Australian Museum*, 23 (4), 309–357. https://doi.org/10.18195/issn.0312-3162.23(4).2007.309-357

Soulebeau, A., Pellens, R., Lowry, P.P., Aubriot, X., Evans, M.E.K. & Haevermans, T. (2016) Conservation of phylogenetic diversity in Madagascar's largest endemic plant family, Sarcolaenaceae. *In*: Pellens, R. & Grandcolas, P. (Eds.), *Biodiversity Conservation and Phylogenetic Systematics, Topics in Biodiversity and Conservation, vol 14. Springer, Cham*, pp. 255–374. https://doi.org/10.1007/978-3-319-22461-9_18

Stephens, M., Smith, N.J. & Donnelly, P. (2001) A new statistical method for haplotype reconstruction from population data. *American Journal of Human Genetics*, 68 (4), 978–989. https://doi.org/10.1086/319501

Sternfeld, R. (1918) Zur Tiergeographie Papuasiens und der pazifischen Inselwelt. *Abhandlungen der Senckenbergischen Naturforschenden Gesellschaft (Frankfurt)*, 36, 375–436.

Sun, J., Liu, W., Guo, Z., Qi, L. & Zhang, Z. (2022) Enhanced aridification across the Eocene/Oligocene transition evidenced by geochemical record in the Tajik Basin, Central Asia. *Global and Planetary Change*, 211, 103789. https://doi.org/10.1016/j.gloplacha.2022.103789

Tamura, K., Stecher, G. & Kumar, S. (2021) MEGA11: Molecular Evolutionary Genetics Analysis version 11. *Molecular Biology and Evolution*, 38, 3022–3027. https://doi.org/10.1093/molbev/msab120

Uchôa, L.R., Delfim, F.R., Mesquita, D.O., Colli, G.R., Garda, A.A. & Guedes, T.B. (2022) Lizards (Reptilia: Squamata) from the Caatinga, northeastern Brazil: Detailed and updated overview. *Vertebrate Zoology*, 72, 599–659. https://doi.org/10.3897/vz.72.e78828

Uetz, P. (2025, editor) The Reptile Database. Available from: http://www.reptile-database.org (accessed February 1st, 2025)

Vences, M., Guayasamin, J.M., Miralles, A. & De la Riva, I. (2013) To name or not to name: Criteria to promote economy of change in Linnaean classification schemes. *Zootaxa*, 3636, 201–244. https://doi.org/10.11646/zootaxa.3636.2.1

Vences, M., Patmanidis, S., Schmidt, J.C., Matschiner, M., Miralles, A. & Renner, S.S. (2024) Hapsolutely: a user-friendly tool integrating haplotype phasing, network construction, and haploweb calculation. *Bioinformatics Advances*, 4 (1), vbae083. https://doi.org/10.1093/bioadv/vbae083

Weppe, R., Orliac, M.J., Guinot, G. & Condamine, F.L. (2021) Evolutionary drivers, morphological evolution and diversity dynamics of a surviving mammal clade: cainotherioids at the Eocene–Oligocene transition. *Proceedings of the Royal Society B*, 28820210173. https://doi.org/10.1098/rspb.2021.0173

Wieczorek, II, P. (2021) *Home Range Area, Overlap, Homing Behavior and Movement Patterns in Plestiodon Reynoldisi*. M.S. Thesis, University of South Florida. Available from: https://digitalcommons.usf.edu/etd/9260 (accessed 1 October 2025)

Wollenberg, K.C., Vieites, D.R., Van Der Meijden, A., Glaw, F., Cannatella, D.C. & Vences, M. (2008) Patterns of endemism and species richness in malagasy cophyline frogs support a key role of mountainous areas for speciation. *Evolution*, 62 (8), 1890–1907. https://doi.org/10.1111/j.1558-5646.2008.00420.x

Zhang, C., Rabiee, M., Sayyari, E. & Mirarab, S. (2018) ASTRAL-III: Polynomial time species tree reconstruction from partially resolved gene trees. *BMC Bioinformatics*, 19, 153. https://doi.org/10.1186/s12859-018-2129-y

Appendices

APPENDIX 1. Additional specimens examined

Grandidierina fierinensis.
MNHN-RA-1895.214, "*Tullear*" (= Toliara), holotype of *Scelotes fierinensis* Grandidier, 1869; MNHN-RA-1905.133, -133A, -133B, -133C, Fiherena plain; MNHN-RA-1979.8269, Vohombe (Betioky); MNHN-RA-1980.1219, 37 km from Betioky, dir. Soalara; MNHN-RA-1983.493, 1983.494, Toliara; ZSM 604/2000 (FG/MV 2000.566), ZSM 605/2000 (FG/MV 2000.567), Toliara, near Arboretum, 28 m a.s.l., 23.40°S, 43.75°E; ZSM 220/2003 (FG/MV 2002.1546), ZSM 225/2003 (FG/MV 2002.1538), ZSM 226/2003 (FG/MV 2002.1595), Toliara, Arboretum; MNHN-RA-1984.410, 1986.57, 1986.58, -59, -60, -61, -62, -63, plain of Toliara, Plantations Pétignat; ZSM 386/2005 (FGZC 2685), near Toliara; MNHN-RA-1984-172, Vobritomotsy, under a kily tree; ZSM 848/2001, Fiherenana river, near Miary; ZSM 1618/2010 (ZCMV 12887), ZSM 1619/2010 (ZCMV 12884), Tombohina, road to Anakao, 23.867333°S, 44.087667°E, 180 m alt; ZSM 1635/2010 (ZCMV 12885), ZSM 1634/2010 (ZCMV 12883), ZSM 1633/2010 (ZCMV 12882), ZSM 1636/2010 (ZCMV 12886), Anakao, hotel chez Emile, 23.655417°S, 43.650139°E; ZSM 606/2000, 607/2000, 608/2000, 609/2000, 610/2000, Anakao, 10 m a.s.l.; MNHN-RA-1929.160, Ampalaza. Unknown locality: MNHN-RA-1979.8270.

Grandidierina lineata.
MNHN-RA-1901.240, "*Ambovombe*", lectotype of *Grandidierina lineata* Mocquard, 1901; MNHN-RA-1901.240-241, "*Ambovombe*", paralectotype of *Grandidierina lineata* Mocquard, 1901; MNHN-RA-1901.174, -175, "*pays Androy sud*", paralectotypes of *Grandidierina lineata* Mocquard, 1901; ZSM 1623/2010 (ZCMV 12891), ZSM 1624/2010 (ZCMV 12845), ZSM 1625/2010 (ZCMV 12850), ZSM 1626/2010 (ZCMV 12847), ZSM 1621/2010 (ZCMV 12894), ZSM 1622/2010 (ZCMV 12893), dunes of Faux Cap, 25.568778°S, 45.531361°E; MNHN-RA-1956.69, Nosy Vorona (Mahafale coast); MNHN-RA-1980.1220 to 1980.1231, 37 km N Betioky, direction to Soalara; MNHN-RA-1980.1232, Ankazomanga; MNHN-RA-1980.1233, Androka, road Ejeda to Beahitsy; MNHN-RA-1980.1234, Egogo; MNHN-RA-1980.1235, Manombo, SWW Beloha; MNHN-RA-1980.1236, Evanga, between Saodona and Bevoalavo; MNHN-RA-1980.1237, Tsivaha, Cap Malaimpioka, S Anjirazato; MNHN-RA-1980.1238, Anjirazato, SW Beloha; MNHN-RA-1980.1239, Besakoa, coast between Faux Cap and Cap Ste Marie; MNHN-RA-1980.1240, Saraondry; MNHN-RA-1980.1241, -1242, Benanoka; MNHN-RA-1980.1243, Ampihany; MNHN-RA-1980.1244, Sakaraha; MNHN-RA-1980.1245, Toliara, base hydro; MNHN-RA-1982.1257, N Toliara, PK32 forest; MNHN-RA-1982.1261, Toliara; MNHN-RA-1984.171, Vobritomotsy; ZSM 611/2000, Anakao. Unknown localities: MNHN-RA-1933.0079 to -0081, MNHN-RA-1930.342, MNHN-RA-1950.396 to -398, MNHN-RA-1970.347.

Grandidierina petiti.
MNHN-RA-1924.91, "*Tsivono, region de Tuléar, à 24 kilometres au Nord de cette ville*", lectotype of *Grandidierina petiti* Angel, 1942; MNHN-RA-1924.90, type locality, paralectotype of *Grandidierina petiti* Angel, 1942; ZSM 1620/2010 (ZCMV 12824), Sakabera, village on the road to Ifaty, on the border of the Fiherenana river, 23.303083°S, 43.658722°E; ZSM 1617/2010 (ZCMV 13009), Ifaty Mangily Reserve, 23.122792°S, 43.609450°E; ZSM 228/2003, Ifaty.

Grandidierina rubrocaudata.
MNHN-RA-7639, «*Fierin*», holotype of *Acontias rubrocaudatus* Grandidier, 1869; MNHN-RA-1979.8268, Befandriana; MRSN R3726 (FAZC 14370 / ACZC 2565), Zombitse; Manioca plantation; ZSM 1630/2010 (ZCMV 12830), ZSM 1629/2010 (ZCMV 12833), ZSM 1632/2010 (ZCMV 12831), ZSM 1628/2010 (ZCMV 12832), ZSM 1631/2010 (ZCMV 12829), Sakabera, village on the road to Ifaty, 23.303083°S, 43.658722°E ; ZSM 232/2003 (FG/MV 2002.2050), Ifaty; ZSM 384/2005, ZSM 385/2005, near Toliara. Unknown localities: MNHN-RA-7795, MNHN-RA-1989.3745.

Paracontias ampijoroensis.
KUZ R069565 (field number AMP2012-parabr, holotype), adult, from Ampijoroa, Ankarafantsika National Park, Mahajanga Province, Madagascar, 16.316926°S, 46.806194°E, 153 m above sea level, collected on 24 January 2012, by H. R. Maheritafika. KUZ R069566 (AMP2012-093, paratype), adult, from a locality very close to the type locality, 16.317526°S, 46.811299°E, 148 m above sea level, collected on 16 January 2012, by H. R. Maheritafika. KUZ R069567 (AMP2012-parawh, paratype), adult, from a locality very close to the type locality, 16.314556°S, 46.818194°E, 89 m above sea level, collected on 2 February 2012, by R. Ito.

Paracontias brocchii.
ZSM 244/2004, Montagne d'Ambre, 12.516667°S, 49.166667°E, ca. 1000 m a.s.l., Antsiranana Province, northern Madagascar.

Paracontias fasika.
ZSM 2256/2007 (holotype), Baie de Sakalava, 12.273334°S, 49.392499°E, 11 m a.s.l., Forêt d'Orangea, Antsiranana Province, northern Madagascar.

Paracontias hafa.
MRSN R1825 (holotype), Anjanaharibe-Sud Massif, Analabe Valley, Campsite W1, Befandriana Fivondronana, Mahajanga Faritany, 14.766667°S, 49.450000°E, 1000–1100 m a.s.l., northeastern Madagascar.

Paracontias hildebrandti.
ZMB 9695 (holotype), "nordwestliches Madagaskar"; ZSM 1578/2008, Montagne des Français, 12.333333°S, 49.366667°E, 120 m a.s.l., northern Madagascar.

***Paracontias holomelas*.**
BM 1946.8.13.69 (lectotype), BM 1946.8.13.67–68 (paralectotypes), Madagascar, "Anzamaharu"; ZMB 14340, Madagascar (probably Akkoraka, central Madagascar; F. Tillack pers. comm.).

***Paracontias kankana*.**
ZSM 1810/2008 (holotype), Mahasoa forest (pitfall camp), near Ambatodisakoana village, 17.297690°S, 48.701990°E, 1032 m a.s.l., eastern Madagascar.

***Paracontias manify*.**
MRSN R1887 (holotype), Antsahamanara, Manarikoba Forest, RNI de Tsaratanana, Marovato Fivondronana, Antsiranana Faritany, 14.042500°S, 48.779833°E, about 1000 m a.s.l., northern Madagascar.

***Paracontias mahamavo*.**
ZSM 2905/2011 (holotype), adult, from Matsedroy, Mahajanga Province, 15.487135°S, 46.646922°E, 27 m above sea level, collected on 30 June 2011, by J. Coates. ZSM 2904/2011, adult, same data as holotype. ZSM 166/2013 (fieldnumber 1RMG14, paratype), adult, from Matsedroy, Mahajanga Province, Madagascar, 15.487135°S, 46°38′48.8″E, 27 m above sea level, collected on 20 July 2013 by M. Rabenoro.

***Paracontias minimus*.**
MNHN 1905.270 (lectotype), MNHN 1905.270A (paralectotype), «Madagascar»; ZFMK 88051–88052, ZSM 2249–2253/2007, ZSM 2268/2007, ZSM 1585–1586/2008, Baie de Sakalava, Forêt d'Orangea, 12.273334°S, 49.392500°E, 11 m a.s.l.; ZSM 1584/2008, south-east of Ivovona, Forêt d'Orangea, 12.273334°S, 49.392500°E; ZSM 1583/2008, Ampombofofo, Babaomby region, 12.098056°S, 49.330278°E, Antsiranana Province, all from northern Madagascar.

***Paracontias rothschildi*.**
ZFMK 88048–88050, ZSM 2074/2007, ZSM 2235/2007, ZSM 2246–2247/2007, ZSM 2260–2269/2007, ZSM 1580–1582/2008, Baie de Sakalava, Forêt d'Orangea, 12.273333°S, 49.392500°E, 11 m a.s.l.; ZSM 1579/2008, south-east of Ivovona, Forêt d'Orangea, 12.332778°S, 49.405556°E, Antsiranana Province, northern Madagascar.

***Paracontias tsararano*.**
MRSN R1787 (holotype), Tsararano Forest, Campsite 1, 14.906665°S, 49.686667°E, 710 m a.s.l., Antsarahan'ny Tsararano, northeastern Madagascar.

***Paracontias vermisaurus*.**
ZSM 597/2009 (holotype), Makira Reserve, site locally named Angozongahy, 15.437027°S, 49.118612°E, 1009 m a.s.l.; ZSM 598/2009 (paratype), Makira Reserve, site locally named Ampofoko, 15.422861°S, 49.120861°E, 1034 m a.s.l.

Voeltzkowia mira.
ZSM 867/0, west Madagascar, collected by Voeltzkow. ZSM 268-272/2023 (ZCMV 15757, 15767, 15768, 15771, 15780), Garden of Mr Blaise (15.573544°S, 46.424206°E), Antsanitia, Boeny region, Northwest of Madagascar, collected on 26 and 27 March 2023 by A. Miralles, N. A. Rahagalala and S. Rakotomanga with the help of local population.

Voeltzkowia mobydick.
UADBA R70487 (field number MA293, ZCMV 12920, holotype of *Sirenoscincus mobydick*), UADBA R70488 (field number MA283, paratype), 3 km from the village of Marosely (15.647139°S, 47.583056°E, 250 m a.s.l.), plateau Bongolava, commune rurale de Port Bergé II, collected by M. Anjeriniaina. ZSM 3207/2012 (field number ZCMV 13587), Plateau de Bongolava, near Boriziny, Camp site, collected on 11 February 2012 by A. Rakotoarison and A. Razafimanantsoa.

***Voeltzkowia shaihulud*.**
ZSM 114/2023 (holotype, field number ZCMV 13724), from the white sand area of the Belambo forest (14.919570°S, 47.762910°E, 116 m a.s.l.), Sofia region, Northwest of Madagascar, collected on 18 October 2023 by A. Rakotoarison, D. Razafimanafo, A. Hasiniaina and A. Razafimanantsoa. UADBA-ZCMV 13723, paratype, same collection data as holotype.

***Voeltzkowia volontany*.**
ZSM 266/2023 (holotype, field number ZCMV 5795, MIRZC 1194), from the white sand area at the summit of the hill nearby Toby Kristy Voahombo (Marovantaza) (15.351299°S, 47.653180°E, ca. 120 m a.s.l.), 3 km north to the village of Marovantaza, Sofia region, North West of Madagascar, collected on 8 April 2023 by local assistants collaborating with A. Miralles, N. A. Rahagalala and S. Rakotomanga.

Voeltzkowia yamagishii.
ZSM 3208/2012 (field number ZCMV 14101), ZSM 3209/2012 (field number ZCMV 14102), Ankarafantsika, 135 m a.s.l., collected on 19 December 2012 by A. Rakotoarison, J. Erens, and E. Rajeriarison.

APPENDIX 2. Substrate preferences of *ZiPa* clade species. Two distinct ecological states were defined: (1) the *psammophilous state* (sand affinity), which includes species typically associated with predominantly mineral, sandy substrates—most often white sand—found in northern and north-western Madagascar, usually in dry deciduous forests or bushy savannah-like vegetations and (2) the *humicolous state* (humus affinity), referring to species primarily found in moist evergreen forests, where they inhabit mainly organic substrates such as decomposing leaf litter.

Species	State	Sources
P. ampijoroensis	psammophilous	Miralles *et al.* 2016a
P. brocchii	humicolous	Glaw & Vences 2007
P. fasika	psammophilous	Köhler *et al.* 2010
P. hildebrandti	psammophilous	Glaw & Vences 2007
P. holomelas	humicolous	Glaw & Vences 2007
P. kankana	humicolous	Köhler *et al.* 2009
P. mahamavo	psammophilous	Miralles *et al.* 2016a
P. manify	humicolous	Andreone & Greer 2002
P. minimus	psammophilous	Köhler *et al.* 2010
P. rothschildi	psammophilous	Köhler *et al.* 2010
P. vermisaurus	humicolous	Miralles *et al.* 2011b
Zig zag	psammophilous	Present work

APPENDIX 3. Models of substrate preference evolution (psammophilous vs. humicolous) tested using HiSSE, implemented in the R package hisse, on the limbless clade comprising *Zig zag* and the genus *Paracontias*. Analyses were conducted on 50 trees randomly sampled from the posterior distribution of the dated phylogeny obtained with BEAST. The table reports the number of trees for which each model was identified as the best-fitting according to AICc weights. The most statistically supported model is indicated in bold. Modeled of observed (0, 1) and hidden states (A, B) are 0A, 1A, 0B, 1B. State 0 (psammophilous); State 1 (humicolous).

Model name	**Model description**	**Number trees best-fitting**
hisse_4p_all_no_dual	**2 hidden states; speciation, extinction, and transition rates variable; dual transitions not allowed**	**50**
BiSSE_like_fit.all	all rates variable	0
BiSSE_like_fit.base	all rates fixed	0
BiSSE_like_fit.fixed_lambda	only extinction and transition rates variable	0
BiSSE_like_fit.fixed_mu	only speciation and transition rates variable	0
BiSSE_like_fit.fixed_q	only speciation and extinction rates variable	0
BiSSE_like_fit.lambda	only speciation rate variable	0
BiSSE_like_fit.mu	only extinction rate variable	0
BiSSE_like_fit.q	only transition rates variable	0
BiSSE_like_fit.q01null	speciation and extinction rates variable; transition 0-1 null	0
BiSSE_like_fit.q01null_INDE	speciation and extinction rates fixed; transition 0-1 null	0
BiSSE_like_fit.q10null	speciation and extinction rates variable; transition 1-0 null	0
BiSSE_like_fit.q10null_INDE	speciation and extinction rates fixed; transition 1-0 null	0
CID_2	BiSSE-like null model	0
CID_4	HiSSE null model	0
hisse_3_2_params_no0B_ alltransitions_no_dual	2 hidden states and 0B combination excluded; speciation and extinction rates 0A-1A fixed; transition rates variable and dual transitions not allowed	0
hisse_3_2_params_no0B_ alltransitions_no_dual_equal	2 hidden states and 0B combination excluded; speciation and extinction rates 0A-1A fixed; transition rates fixed and dual transitions not allowed	0

.....continued on the next page

APPENDIX 3. (Continued)

Model name	Model description	Number trees best-fitting
hisse_3_2_params_no1B_ alltransitions_no_dual	2 hidden states and combination 1B excluded; speciation and extinction rates 0A-1A fixed; transition rates variable and dual transitions not allowed	0
hisse_3_2_params_no1B_ alltransitions_no_dual_equal	2 hidden states and combination 1B excluded; speciation and extinction rates 0A-1A fixed; transition rates fixed and dual transitions not allowed	0
hisse_3differentp_no0B_ alltransitions_no_dual	2 hidden states and 0B combination excluded; speciation, extinction, and transition rates variable; dual transitions not allowed	0
hisse_3differentp_no0B_ alltransitions_no_dual_equal	2 hidden states and 0B combination excluded; speciation and extinction rates variable; transition rates fixed and dual transitions not allowed	0
hisse_3differentp_no1B_ alltransitions_no_dual	2 hidden states and combination 1B excluded; speciation, extinction, and transition rates variable; dual transitions not allowed	0
hisse_3differentp_no1B_ alltransitions_no_dual_equal	2 hidden states and combination 1B excluded; speciation and extinction rates variable; transition rates fixed and dual transitions not allowed	0
hisse_4p_equal_no_dual	2 hidden states; speciation and extinction rates variable; transition rates fixed and dual transitions not allowed	0